IET Nanobiotechnology

Review Article

IET Journals
The Institution of Engineering and Technology

Antibacterial magnetic nanoparticles for therapeutics: a review

ISSN 1751-8741
Received on 13th April 2019
Revised 24th June 2019
Accepted on 10th July 2019
E-First on 29th August 2019
doi: 10.1049/iet-nbt.2019.0146
www.ietdl.org

Alireza Allafchian[1] ✉, *Seyed Sajjad Hosseini*[1]

[1]*Research Institute for Nanotechnology and Advanced Materials, Isfahan University of Technology, Isfahan 84156–83111, Iran*
✉ *E-mail: allafchian@cc.iut.ac.ir*

Abstract: Along with the extensive range of exotic nanoparticle (NPs) applications, investigation of magnetic NPs (MNPs) *in vitro* has ushered modern antibacterial studies into an increasingly attractive research area. A great number of microorganisms exist in the size scales from nanometre to micrometre regions. The enormous potential of engineered MNPs in therapeutic procedures against various drug-resistant bacteria has declined the menace of fatal bacterial infections. Many biocompatible MNPs have been introduced that possess remarkable impacts on various bacterial strains. Conventional synthesis methods such as co-precipitation or hydrothermal techniques have been widely adopted in the production of MNPs. The MNPs for antibacterial applications are mainly required to be superparamagnetic, recyclable and biocompatible. To implement novel strategies in developing new generation antimicrobial magnetic nanomaterials, it is essential to obtain a comprehensive preview of recent achievements in synthesis, proposed antibacterial mechanisms and characterisation techniques of these nanomaterials. This review highlights notable aspects of antibacterial activity in engineered MNPs and nanocomposites including their particle properties (size, shape and saturation magnetisation), antibacterial mechanisms, synthesis methods, testing methods, surface modifications and minimum inhibitory concentrations.

1 Introduction

1.1 Motivation

Today, despite remarkable achievements in treating infectious diseases, the perceived threat to public health has increased due to facilitated travelling around the world and expanded global interconnections. As emphasised in a 2018 report by World Health Organization (WHO), next to human immunodeficiency virus/acquired immune deficiency syndrome, tuberculosis is one of the two leading infectious causes of death threatening around 10,000,000 people each year who fall ill due to an infection by *Mycobacterium tuberculosis* [1]. In 2009, many lives were endangered across 74 countries by influenza A H1N1 which was identified as a swine-mediated pandemic and was introduced as a public health emergency of international concern by WHO [2, 3]. Infections caused by bacterial pathogens are one of the major threats to human health. Antibiotics are generally known as a proper treatment against bacterial infections. However, much of the bacterial multi-drug resistance stems from an imprudent use of antibiotics in spite of their long clinical success. An increasing rate of microbial resistance to previously developed medical treatments adds further complications to control epidemics. This has propelled to the forefront an ongoing research attempt to discover alternative efficient therapies.

In a general sense, antibacterial agents can be categorised into organic and inorganic classes [4]. Medicinal plants are among remarkable examples of organic antibacterial materials [5], and metal oxide nanoparticles (NPs) have proved effective in providing antibacterial properties as inorganic agents [6]. Recent developments in NP applications have highlighted the need for innovative approaches in treating bacterial infections. Optimisation of antibacterial performance mediated by NPs is a major area of interest within the field of novel antibacterial therapeutics. Among investigated antibacterial NPs, magnetic NPs (MNPs) stand out essentially due to their response to external magnetic fields. Their magnetic character has enabled them to offer a wide variety of biomedical applications from diagnostics to *in vivo* therapeutic methods [7].

1.2 Therapeutic NPs

In the area of inorganic therapeutic medicine, metal NPs have leveraged the efficiency of antibacterial nanoagents across both preclinical and clinical studies [8–13]. Additionally, the antibacterial function of NPs has ensured their wide application in a rich variety of therapeutic techniques [14–16]. Silver (Ag) NPs have so far received considerable attention in producing a new class of antimicrobials giving rise to novel approaches in the treatment of bacterial infections. The effectiveness of using Ag in the therapeutic intervention of NPs has been thoroughly exemplified in a review by Franci *et al.* [17].

Precisely tunable photothermal and optical properties of gold (Au) NPs have made them one of the most widely investigated metal NPs. Also, it is observed that they can enhance X-ray radiotherapy in subcutaneous mammary tumour treatment in mice [18]. Moreover, the inherent limitations of traditional cancer therapies stimulated the development of various methods using nanotechnology for enhancing cancer treatment as well as reducing the accompanied side effects. Phenomenal success has been achieved by incorporating nanotherapy in local treatment of tumours in organs as susceptible as the brain [19, 20]. Despite its safety and efficacy, medical nanotechnology suffers from a few drawbacks in this area including the complexity of tumour microenvironment along with its heterogeneity, an incomplete understanding of related chemistry and control parameters over the preparation process, clinical translation and commercialisation.

Development of magnets in various shapes and sizes has extensively suggested novel investigations in incorporating MNPs into various therapies. Diagnostic capability of iron-oxide NPs due to their magnetic properties has brilliantly contributed to tumour detection methods [21]. In a magnetic resonance imaging scan, the iron-oxide NPs can yield enhanced images once they attach to tumour cells [22]. Attachment to tumour cells in the bloodstream is also regarded as a privilege of MNPs, where they can be used as a cancer diagnosis tool [23]. Hyperthermia approaches using iron-oxide NPs have also been influential in the field of cancer treatment because of their higher specific absorption rate [24].

The introduction of superparamagnetic NPs to medicine has triggered a considerable amount of research in recent developments

of both *in vivo* and *in vitro* medical treatments [25]. The pioneering work in implementing magnetic particles in treatments included the use of carbonyl iron particles in a magnetic field for obstructing intracranial aneurysms [26]. Furthermore, magnetic drug targeting has been established as a novel method in local treatment of tumours. Doxorubicin-loaded dendritic-Fe_3O_4 supramolecular NPs administered into the tumour supplying artery of tumour-bearing mice have provided significant tumour regression and has successfully captured its further growth [27].

1.3 Antibacterial MNPs

The activity of NPs may generally be classified on the basis of their mechanism of action against bacteria into growth inhibition (bacteriostatic) [28] or killing (bactericidal) [29] activities. Owing to a variety of mechanisms discussed in the following sections, the majority of MNPs possesses a bactericidal character as applied against both Gram-positive and Gram-negative bacteria (see Table 1 of results).

Iron MNPs benefit from a number of advantages over other NPs [45] including an inexpensive synthesis, feasible large-scale production, biocompatibility and environmental safety. The bacterial inhibitory activity of MNPs can be illustrated in the area of water disinfectants, where they would benefit from the magnetic character of iron-oxide NPs as by introducing them into the polymerisation process of thiourea and formaldehyde [46], and thus providing a promising regression activity against bacterial and fungal activities in the aqueous environment.

Catalysed reduction of dye-contaminated water has also been achieved by means of metal-deposited magnetic catalyst microspheres, which are comprised of amino-functionalised Fe_3O_4–silicon dioxide (SiO_2) core–shell structures [47].

Markiewicz *et al.* [48] investigated the bactericidal effect of a polymer/Au/MNPs nanohybrid that can effectively inhibit the metabolic activity of planktonic *Pseudomonas aeruginosa* as well as preventing its biofilm formation. Au coatings can improve the stability and biocompatibility of MNPs [49], and polymers can allow a facile control of chemical composition in a shell.

On the basis of several antimicrobial studies conducted on MNPs, many of them have been fabricated in a core–shell structure while reports of bare MNPs active against bacteria have also been published (see Table 1 of results). Nickel oxide (NiO) NPs have shown favourable bacterial growth inhibition by distracting the cell membrane, which results in the disruption of cell enzymes [50]. It was also found that superparamagnetic Ni colloidal nanocrystal clusters may introduce novel inherent properties for antibacterial applications as they can provide tunable particle sizes and magnetic moments [51].

A large number of plants are rich in minerals [52] and can be used for the green synthesis of MNPs. In addition, the incorporation of plant extracts in the antibacterial performance of MNPs has been successfully established [53]. Over the past centuries, many plants have been introduced in traditional medicine practises to treat diseases and infections. They are known to possess a wide variety of medicinal properties such as their antibiotic, antioxidant and wound healing qualities [54, 55]. *Couroupita guianensis* leaves, for instance, are traditionally known as the cure for skin diseases and malaria [56, 57].

In this review, we aim to focus on the antibacterial character of MNPs with therapeutic potential, an overview of their antibacterial mechanisms and a brief description of popular assays to analyse their antibacterial effects together with their selected characteristics such as morphology and magnetic response.

Table 1 List of common magnetic antibacterial NPs

MNPs	Coated/ doped with	Size[a], nm	M_s[b], emu g^{-1}	Synthesis method	Mechanism	Target bacteria	Reference
Fe_3O_4	Silica	10/53 (DLS)	Fe_3O_4:55 Fe_3O_4–SiO_2:40.90	co-precipitation	radio-frequency-mediated physical perturbation of cell membranes and bacterial membrane dysfunction	*E. coli* *S. aureus*	[30]
$Ni_{1-x}Nd_xO$	Nd^{3+}	28 nm (XRD) (for $x = 0.03$)	0.03 (for $x = 0.03$)	co-precipitation	reaction of Ni^{2+} with sulphydryl groups inside the cell and damaging synthetase activity in the microbe	*S. aureus* *Klebsiella pneumonia* *Shigella dysenteriae* *E. coli* *Proteus vulgaris*	[31]
calcium Fe_2O_4	chitosan–ampicillin	25 (XRD)	0.114	solution combustion method	ampicillin release from chitosan with CFNP	*Staphylococcus epidermis*	[32]
$CuFe_2O_4$	Ag–tannic acid–papain	29.3/46.2 (XRD)	57.8/62.1	solvothermal	increased the membrane permeability and acting on the proteins and the peptidoglycan of the cell wall	*E. coli* *S. aureus*	[33]
$La_{1-x}Na_yMnO_3$	silica	48/47 (XRD)	29/34	sol–gel	electrostatic attraction to the negative moieties in the bacteria membrane	*Micrococcus varians* *Bacillus spp* *Serratia spp* *Aspergillus spp*	[34]
Fe_3O_4	$Ba_3(PO_4)_2$	Fe_3O_4: 100 (TEM) nanoflakes: 40 nm × 7 µm	8.7	solvothermal	destruction of cell integrity by altering cell permeability and protein oxidation due to ROS generation	*E. coli*	[35]
Fe_3O_4	MOR and CuO	Fe_3O_4: 16.6 mordenite (MOR): 18.43 CuO: 12	Fe_3O_4: 73.65 Fe_3O_4@MOR: 8.3 Fe_3O_4@MOR@CuO: 4.2	solvothermal	binding of Cu^{2+} ions to the functional groups of proteins and enzymes, which causes inactivation and inhibition in cell processes	*E. coli* *S. aureus*	[36]

MNPs	Coated/doped with	Size[a], nm	M_s[b], emu g^{-1}	Synthesis method	Mechanism	Target bacteria	Reference
Fe_3O_4	thiourea–formaldehyde polymer, Ag^+, Au^{3+}	10–50 (DLS)	magnetic thiourea-formaldehyde (MTUF): 45.54 MTUF-Ag: 31.57 MTUF-Au: 35.89	co-precipitation	reaction of Ag(I) or Au (III) ions with amino and/or thiol groups on the thiourea moiety and damaging cell membrane	*E. coli* *Salmonella typhimurium* *S. aureus* *Listeria monocytogenes* *Candida albicans*	[37]
$CoFe_2O_4$	Okra (*Abelmoschus esculentus*) plant extract	55 (XRD) 5–50 (DLS)	65.31	green synthesis with microwave heating methods	production of ROS and accumulation of NPs in the cytoplasm or on the outer membranes	*Enterobacter aerogenes* *Yersinia enterocolitica* *S. aureus* *Micrococcus luteus*	[38]
NiO	—	8.15 (XRD) 8–10 (HRTEM)	not saturated	green synthesis using *Aegle marmelos* extract	increased electrostatic attraction between the microbial cell membrane and Ni ions	*S. aureus* *Streptococcus pnemoniae* *E. coli* *Escherichia hermannii*	[39]
Fe_3O_4	PEG	46.2/35.7	Fe_3O_4: 56.43 Fe_3O_4: 74.33	co-precipitation	oxidisation of bacteria assisted by the hydrophilic properties of PEG	*E. coli* *S. aureus*	[40]
$AgXO_2$	X = Fe, Cr	$AgFeO_2$: 48.8 (XRD), 80.4 (HRTEM) $AgCrO_2$: 77.1 (XRD), 120.9 (HRTEM)	$AgFeO_2$: 1.1244 $AgCrO_2$: 0.18978	flash auto-combustion reaction	formation of the free radical species from the Ag ions	*Bacillus subtilis* *S. aureus* *Streptococcus faecalis* *E. coli* *Neisseria gonorrhoeae* *P. aeruginosa*	[41]
ZnO	La	ZnO: 16.35 (XRD) ZnO/La (0.07 M): 9.75 (XRD)	ZnO/La (0.07 M): ~0.006	wet-chemical method	creation of active species by photoinduced reaction	*B. subtilis* *S. aureus* *Proteus mirabilis* *Salmonella typhi*	[42]
$TbVO_4$	—	30–50 (SEM)	0.52	co-precipitation	interaction of NPs with the outer membrane of bacteria and arresting the respiration pathway	*E. coli* *S. aureus*	[43]
ZnO	Co (5%)	ZnO/Co: 40 (XRD), 60 (SEM), 32–76 (DLS) ZnO: 35 (XRD), 65 (SEM), 42–90 (DLS)	0.00465	wet-precipitation method	improved (enhanced) binding forces and generation of free radicals in cell	*S. dysenteriae* *Vibrio cholera* *E. coli*	[44]

Coated materials together with the obtained values of size and saturation magnetisation (M_S), synthesis methods and proposed antibacterial mechanisms of various MNPs against a variety of pathogenic bacteria are presented.

[a]Column indicates the sizes of final coated or functionalised NPs, and if available, the sizes of bare core NPs are separated by a slash (/); the size measurement methods have been mentioned in parentheses, where (XRD) denotes the obtained crystallite size from an XRD pattern.

[b]Values of saturation magnetisation are measured at room temperature.

2 Antibacterial MNPs synthesis methods

2.1 Synthesis of MNPs

A number of effective methods to synthesise MNPs have been introduced including both aqueous and non-aqueous-based routes. Co-precipitation technique [30], hydrothermal method [58], microemulsion approach [59], sol–gel process [34] and sonochemical synthesis [60] are among the aqueous methods and thermal decomposition method [61], spray pyrolysis [62] and polyol-induced solvothermal [63] process are examples of non-aqueous synthesis procedures (Fig. 1).

In a recent study, Sathish Kumar *et al.* [64] used a green synthesis route to obtain iron-oxide MNPs. In this method, Fe_3O_4 NPs were synthesised by a co-precipitation method, where Fe^{3+} ions are reduced in an aqueous solution of *C. guianensis* extract. An extensive review of green synthesis routes for producing Fe_3O_4 NPs has been provided by Yew *et al.*[65], where applications of plant extracts from leaf, fruit peel, seed, stolon and root, gum and plant waste in the synthesis process have been comprehensively categorised and studied.

The synthesis procedures of MNPs can strongly affect their properties, which can be tuned for various applications. Owing to

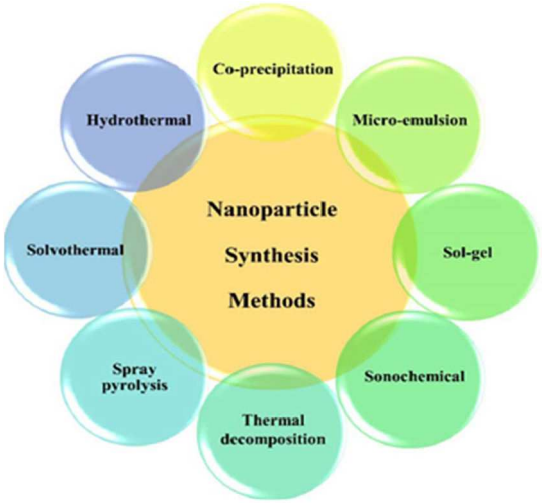

Fig. 1 *Synthesis methods commonly used for preparing MNPs*

its feasibility, aqueous co-precipitation method has been regarded as the most popular idea in the synthesis of iron-oxide NPs (see Table 1 of results). The strategy used to control the size of NPs in this method is to optimise factors such as precursor salt types, ferric/ferrous salts mole ratio and reaction parameters such as pH and temperature [66].

Previous studies have reported that uncoated superparamagnetic iron NPs that have a size below 10 nm can be produced in colloidally stable solutions and control of initial iron concentration allows the synthesis of equivalently sized NPs [67]. Also, core–shell structures comprised of iron-oxide cores and amorphous silica shells are typically synthesised by a sol–gel technique, where the thickness of the silica shell (10–100 nm) can be adjusted by controlling the silane concentration [68].

2.2 Functionalisation methods

Polymeric modification of surface in MNPs can inhibit non-specific adsorptions on them. For instance, in the case of iron-oxide NPs, polyethylene glycol (PEG) functionalisation is able to effectively assist their molecular recognition processes by minimising the adsorption effect [69].

As reported in previous studies, chitosan could be functionalised by a variety of methods including etherification, esterification, grafting and coupling with amines or acids [70]. In a recent study [71], Fe_3O_4–titanium dioxide (TiO_2) NPs were functionalised with methylpyrazolone via a cross-link provided by chitosan which creates a modification opportunity by its both -OH and $-NH_2$ groups.

One of the earliest and most feasible methods to modify NPs is blending, which is achieved by mixing two or more components via physical methods such as stirring [72] or shaking [73]. Modification of functional groups in a compound is commonly termed as a chemical modification. There are several methods to chemically modify a nanomaterial, in which we can make use of chemical reactions [74], radiation [75], photochemical reactions [76], plasma [77] and laser-induced [78] functionalisation and enzymatic grafting [79] methods. Chemical modification of surface in NPs has brought about a vast area of excellent applicability of these materials from efficient drug delivery to surface plasmon effect.

2.3 Antibacterial magnetic nanocomposites

Although various remarkable nanoscale capabilities such as magnetic response, antibacterial effect and feasible recyclability are found among nanoagents, their clinical translation profoundly suffers from their separated functions. As a result, a lack of multifunctional nanomaterials bearing these capabilities combined in one nanosystem has existed as a problem for several years. Optimised composite NPs have been synthesised and presented in the survey to find such nanomaterials as they are capable of being employed in multifunctional applications in nanoscience and exhibit several features synergistically. The excellent antibacterial effects of AgNPs combined with great magnetic response of iron-oxide NPs in a nanocomposite antibacterial system is a phenomenal example of such multifunctional nanomaterials [80]. Table 2 presents a list of recently synthesised magnetic antibacterial nanocomposites together with some of their selected physical features, synthesis methods and their target bacteria.

In the area of novel antibacterial nanocomposite materials, degradation of killing *Escherichia coli* bacteria has been observed through the photocatalytic ability of magnetic cobalt ferrite ($CoFe_2O_4$)/Ag/Ag_3 vanadium oxide (Ag_3VO_4) nanocomposites, and it has been proved that they show a better photocatalytic activity than pure Ag/Ag_3VO_4 and $CoFe_2O_4$ [88]. In addition, the genotoxicity of both uncoated and coated magnetic nanocomposites has led to a renewed interest in biomedical applications of next-generation magnetic nanomaterials. In a recent study [89], L-cysteine and polyacrylic acid-coated ferric Co boron NPs have modulated cytotoxic and genotoxic effects on human dermal fibroblasts and proved to be inducing a remarkable extent of DNA damage to bacteria.

3 Antibacterial activity of MNPs

3.1 Effect of size

Size of NPs could be considered as a measure of their capability to readily enter the intracellular space, as it is presumed that NPs with an average diameter above 40 nm cannot passively penetrate the cell membrane [90]. Jose Ruben *et al.* [91] found that AgNPs synthesised in a range of diameters exhibit a size-dependent antibacterial activity, as direct interaction with Gram-negative bacteria takes place preferentially, where the size of NPs does not exceed 10 nm. In addition, the antimicrobial activity of metal NPs is believed to be a function of their effective surface area, which is increased in smaller-sized NPs, as it is found in a study by Auffan *et al.* [92] that iron-based NPs exhibit size-dependent inhibitory effect against *E. coli*.

In another study, Digigow *et al.* [93] prepared silica-coated MNPs by co-condensating 3-aminopropyltriethoxysilane (APTES) and tetra-ethyl orthosilicate (TEOS) in the presence of superparamagnetic iron-oxide NPs (SPIONs) and observed that the thickness of silica layer directly affects magnetisation of the MNPs. An analogous result is also obtained by Kralj *et al.* [94], where a diminished magnetisation takes place by the incorporation of thicker silica shells.

The nucleation, growth and coarsening kinetics in the synthesis of MFe$_2$O$_4$ NPs (M = Co, Li, Ni, or Mn) have been identified as major contributing factors for achieving NPs with uniform size and shape [95]. The optimum results seem to be obtained if these processes are executed separately in time, i.e. the growth of nuclei must begin only after the end of nucleation process, and the coarsening step has to take place after the growth of nuclei is over. Also, the homogeneity of the solution is a deciding factor in yielding feasibly controlled sizes and shapes.

3.2 Effect of shape

As mentioned above, the impact of size on antibacterial properties and cellular uptake of various spherical NPs has been widely elucidated. However, studies of NP properties show the importance of particle shape in establishing desired antimicrobial and biological performance [96–99]. Moreover, it is thought that engineered NPs with different shapes can be adopted in targeting specific cells [100].

While the influence of particle shape on the antibacterial properties of AgNPs is evident [101], shape-dependent inhibition of bacteria by MNPs are still being investigated. Aside from conventional spherical NPs, particles with other morphologies have also been studied for their antibacterial properties. Efficiently synthesised NiO nanorods with an average diameter of 60 nm exhibited considerable antibacterial activity against *E. coli*, *P. aeruginosa* and *Staphylococcus aureus* [102]. Among other Ni-based antibacterial nanosystems are NiO nanotubes [103] and

NiO/TiO_2 composite nanofibres [104], which would favourably inhibit the viability of a variety of bacterial strains compared with conventional NiO and NiO nanoflowers. Additionally, it is found that Ni-doped zinc oxide (ZnO) nanorods possess remarkable antibacterial potency and are able to completely eradicate the above-mentioned multi-drug-resistant bacteria [105]. Furthermore, crystalline Co molybdate ($CoMoO_4$) nanorods/nanowhiskers with a diameter range from 10 to 80 nm have been successfully tested against *E. coli* [106].

3.3 Functionalisation of MNPs

Although bare MNPs exhibit excellent antibacterial properties, the developed bacterial multi-drug resistance due to repeated application of antibacterial agents calls for more efficient strategies to battle bacterial infections. In this way, surface functionalisation of MNPs for targeting specific cells has provided the opportunity to enhance their efficacies against pathogenic microbes. Cancer treatment is one of the prominent applicability of targeted drug delivery methods, where MNPs would play a key role. In a recent study, the anticancer drug doxorubicin was conjugated with iron-oxide NPs to induce desirable cytotoxicity to the treated cancer

Table 2 List of common magnetic antibacterial nanocomposites

Nanocomposite	Size[a], nm	M_s, emu g^{-1}	Synthesis method	Mechanism	Target bacteria	Reference
β-$CoMoO_4/Co_3O_4$	β-$CoMoO_4$: 20.3 (XRD) Co_3O_4: 33.81 (XRD)	12.063	co-precipitation	ROS generation	*E. coli* *P. aeruginosa* *S. aureus*	[81]
α-Fe_2O_3/Co_3O_4	25.34 (XRD)	82.49	co-precipitation	increasing the overall count of oxygen free radicals produced as a result of the interaction of cytoplasmic water with the composite samples inside the bacterial cell	*B. subtilis* *S. aureus* *E. coli* *S. typhi*	[82]
GO@$CoFe_2O_4$@ Ag-CFX	$CoFe_2O_4$: 16 (XRD) AgNPs: 15 (XRD)	$CoFe_2O_4$: 58.022 GO@$CoFe_2O_4$@Ag-CFX: 37.357	co-precipitation	affecting the cell wall structure	*S. aureus* *B. subtilis* *E. coli* *P. aeruginosa*	[83]
GO-Fe_3O_4@NPVP-Ag	low pH: 700 (DLS) Fe_3O_4: 15 (TEM)	Fe_3O_4: 71.9 GO-Fe_3O_4@NPVP-Ag: 12.7	co-precipitation	immobilised AgNPs on the surface of the GO nanosheets can release Ag + into the interior of bacterial cell	*E. coli* *S. aureus*	[84]
Fe_3O_4@PTA@Ag	250 (HRSEM)	55.47	solvothermal	reaction of oxygen species generated by AgNPs with the cell membrane	*E. coli* *S. aureus*	[80]
Fe_3O_4@C@MgO-Cu	Fe_3O_4: 15 (TEM) Fe_3O_4@C@MgO-Cu: 50 (TEM)	Fe_3O_4: 30.08 Fe_3O_4@C@MgO-Cu: 29.07	co-precipitation hydrothermal	Enhanced physical interaction between the MgO-Cu NP and cell membranes well as the serious damage of cells caused by the increased ROS	*E. coli* *S. aureus*	[85]
TiO_2/Fe_3O_4/chitosan/ methylpyrazolone	agglomerated (TEM)	21	solvothermal	penetration of cell membrane and inactivation of its constituents	*E. coli* *S. aureus* *A. flavus* *C. albicans*	[71]
Fe_3O_4@APTES–EDTA@Ag	50 (XRD) 45 (TEM)	Fe_3O_4: 70 Fe_3O_4@APTES–EDTA: 66 Fe_3O_4@APTES–EDTA@Ag: 57	co-precipitation	facilitated AgNPs uptake through the cell wall by EDTA and increased the formation of free radicals by AgNPs when encapsulated into the EDTA	*E. coli* *S. typhimurium* *S. aureus* *Bacillus cereus*	[72]
$Co_{0.3}Zn_{0.7}Fe_2O_4$/OBM/ Ag	$Co_{0.3}Zn_{0.7}Fe_2O_4$: 65 (XRD) Ag: 10 (XRD)	$Co_{0.3}Zn_{0.7}Fe_2O_4$/OBM: ~15 $Co_{0.3}Zn_{0.7}Fe_2O_4$/OBM/Ag: ~11	sol–gel	formation of free radicals by AgNPs in contaminated water	*S. aureus* *B. cereus* *E. coli* *S. typhimurium*	[86]
$NiFe_2O_4$@PAMA@Ag	$NiFe_2O_4$: 42 (XRD)	$NiFe_2O_4$: 64.8 $NiFe_2O_4$@PAMA@Ag: 49.5	citrate–gel	increasing the available surface area of AgNPs for direct contact to bacteria	*S. aureus* *B. cereus* *E. coli* *S. typhimurium*	[87]

[a]Column contains sizes of final coated or functionalised NPs; the size measurement methods have been mentioned in parentheses, where (XRD) denotes the obtained crystallite size from an XRD pattern.

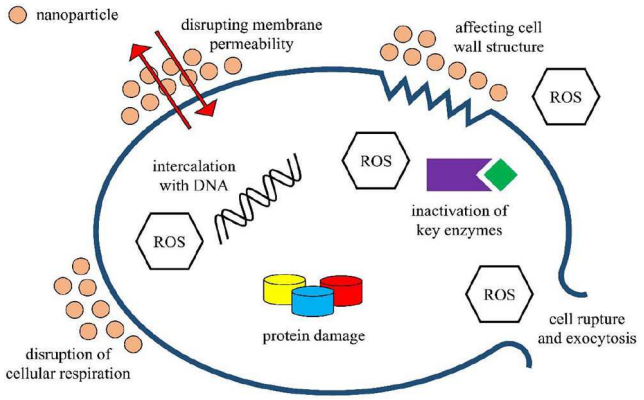

Fig. 2 *Antibacterial mechanisms of MNPs*

cells [107]. As an antibacterial application, tryptophan, an essential amino acid, was loaded on Fe_3O_4 NPs to induce an enhanced performance against bacteria [108].

4 Antibacterial mechanisms of MNPs

There have been several studies published recently regarding the effects of MNPs on a variety of Gram-positive and Gram-negative bacteria (see Tables 1 and 2 for tables of results); however, what is not yet completely clear is their antibacterial mechanisms when applied either *in vitro* or *in vivo*.

The bacterial cell membrane is generally composed of two essential structures, i.e. the cytoplasmic membrane and the cell wall. The major cellular function of the cytoplasmic membrane is selective permeability by which it is able to control the nutritional intake and cellular waste disposal [109]. A phospholipid bilayer with integrated proteins comprises of the cytoplasmic membrane forming about 10 nm thick gate to the intracellular space. In a bacterial phospholipid molecule, an ester linkage bonds fatty acids to a glycerol molecule, which along with phosphate and another functional group (e.g. sugars or ethanolamine) establishes a hydrophilic end in the outer surface of cytoplasmic membrane architecture [110]. The fatty acids of phospholipid molecules point toward each other in the inner region of the cytoplasmic membrane and form a hydrophobic internal area, whereas the outer hydrophilic surface is exposed to the cytoplasmic region on one side and the cell wall on the other side of the membrane. The cell wall outside the cytoplasmic membrane is a rigid barrier that protects the cell against osmotic cell lysis [111]. Peptidoglycan is an essential polysaccharide layer found in the cell wall structure of both Gram-positive and Gram-negative bacteria and ensures the strength and rigidity of the cell wall [112]. The peptidoglycan layer consists of glycan tetrapeptides as its basic units that are connected by peptide cross-links and eventually form a strong surface around the cell. To date, there have been more than 100 chemically distinct peptidoglycans identified with their various peptide groups while their glycan portion remains universal.

Gram-positive cell walls are mainly composed of a thick peptidoglycan layer constructed by several stacks of peptidoglycan monolayers. On the other hand, Gram-negative bacteria devote a much smaller portion of their wall structure to the peptidoglycan layer as they benefit from lipopolysaccharide (LPS) outer membrane as the major part of their cell wall, which is anchored to the peptidoglycan layer by Braun lipoproteins. The LPS layer does not provide the cell with much structural strength, yet it is effectively responsible for blocking many harmful substances such as lipophilic antibiotics. In fact, part of the reason why some antibiotics that inhibit Gram-positive bacteria would render ineffective against Gram-negative bacterial species is explained by the LPS layer function [113].

4.1 Cell membrane destruction

It is believed that electrostatic forces can cause NPs to bind to the bacterial cell membrane and disorganise its metabolic functionality [114]. Damage undertaken by cell membrane may eventually lead to a membrane rupture and leakage of intracellular components including genetic materials and minerals along with vital lipids and proteins. It is found that the antibacterial mechanism of AgNPs is linked to the formation of free radicals that damage the bacterial membrane [86].

Additionally, as the bacterial membrane is depolarised by reactive oxygen species (ROS), it undergoes damage and deformation [115]. It is found that on the interaction of iron-oxide NPs with bacteria, the membrane depolarisation is catalysed. A great deal of cell membrane disruption is induced by pyrrhotite nanostructures, where sharp edges and vertices present on their surface play a significant role in damaging the cell membrane structure [116]. Christena *et al.* [117] found that copper (Cu) NPs are potentially able to inhibit bacterial efflux pump and cause cell death by damaging the cell membrane. Moreover, it is generally agreed that positive charges supplied by primary amine groups of chitosan would readily interact with negatively charged components of the exterior cell wall. This would bring significant changes to the cell surface and disorganise cell permeability, which may effectively result in a leakage of intracellular substances [118].

4.2 ROS generation

Production of ROS is generally one of the natural outcomes of cellular respiratory activity in living organisms [119]. However, it is known that abundant ROS in contact with the cellular environment leads to a disruption of many vital components such as lipids, proteins and DNA [58]. In terms of antibacterial ROS mechanism, superoxide anion (O_2^-), hydrogen peroxide (H_2O_2) and hydroxide (OH^-) radicals are primarily responsible for damaging vital proteins and disruption of DNA molecules in bacterial cells. Many authors propose that the generation of ROS is regarded as the dominant bactericidal mechanism employed by various antibacterial NP agents (Fig. 2).

Photogeneration of ROS on the surface of metal NPs has been suggested in many studies [120, 121]. Moreover, it is believed that the overgeneration of ROS brings a considerable increase in lipid peroxidation and protein oxidation [122]. Also, highly peroxidised lipids will induce an oxidative degradation of polyunsaturated lipids. As a result, the plasma membrane will be damaged, which leads to a membrane leakage [123].

In terms of ROS permeability of bacterial cell membrane, it is found that both Gram-positive and Gram-negative bacteria are equally permeable to ROS [116], the only difference being in ROS intracellular effects. Superoxide and H_2O_2 species are generated in the cytoplasm as a result of oxygen interaction with redox enzymes possessing flavin groups [124]. Superoxide dismutase is an enzyme that catalytically contributes to the dismutation of reactive superoxide to O_2 or H_2O_2 [116]. It is established that a great deal of microbial cell damage can be induced by both superoxide and H_2O_2 species. Pal *et al.* [101] noted that in disrupting bacterial metabolism, AgNPs release Ag ions that are able to inhibit respiratory enzymes, which in part leads to excessive production of ROS.

4.3 Photocatalytic effect

Photocatalytic properties of nano-sized materials have contributed to the process of microbial inhibition and restriction of bacterial biofilm formation. In these materials, the incident light is able to overcome the energy band gap barrier of the NP and consequently produce electron–hole pairs. In a biological context, free electrons are prone to induce ROS and bacterial death.

Previous studies have reported the photocatalytic activity of iron sulphides and their application in biomedical fields and degradation of organic dyes [125]. It is reported that formation of hydroxyl radicals is more efficiently catalysed by iron sulphides compared with ferrous iron [126]. In another study on $CuFe_2O_4@C_3N_4$ core–shell photocatalysts, Yao *et al.* [127] found superior results of photoinduced electron–hole pairs originated in the heterojunction between the interfaces of g-C_3N_4 and $CuFe_2O_4$.

Moreover, the role of TiO_2 NPs in increasing lipid peroxidation when interacting with the cell membrane is explained by its inherent photocatalytic behaviour, which triggers a membrane rupture, inhibited cellular respiration function and eventually cell death [128]. Also, it is found that the antimicrobial activity of AgNPs is enhanced when incorporated in Ag–TiO_2 nanocomposites [129]. In a study conducted by Rawat *et al.* [130], the photocatalytic reactivity of TiO_2-coated $NiFe_2O_4$ MNPs is attributed to the generation of highly active hydroxyl radicals (–OH) which has significantly reduced the concentration of *E. coli* bacteria in Luria-Bertani culture media. Moreover, it is demonstrated that Fe_3O_4@TiO_2 core–shell MNPs have the potential of targeting and inhibiting various drug-resistant pathogenic bacteria such as *Staphylococcus saprophyticus*, *Streptococcus pyogenes* and *S. aureus* [131].

4.4 Cytotoxicity of antibacterial MNPs

Promising results have been reported on the antibacterial effects of MNPs with their possible safe applications *in vivo*. A concise overview of *in vivo* therapeutic capability of iron-oxide NPs is provided by Rodrigues *et al.* [7], where they discuss drug delivery application, biodistribution and toxicity of iron-oxide NPs. A recent study has reported a negligible toxicity of magnetic metallopolymer-grafted NPs to red blood cells and their minimal tendency to induce resistance in bacteria [132]. These recyclable magnetic iron-oxide NPs are grafted with charged cobaltocenium-containing metallopolymers through a reversible addition-fragmentation chain transfer polymerisation method. It is observed that the conjugation of these metallopolymers with β-lactam antibiotics has significantly improved their vitality against both Gram-positive and Gram-negative bacteria. The cytotoxic effect of MNPs on mammalian cells covers an extended area of recent research. Cell viability tests such as 3-4,5-dimethylthiazol-2-yl-2,5-diphenyltetrazolium bromide (MTT) provide information about cytotoxicity. Other studies have suggested that bare iron-oxide NPs demonstrate a biocompatible character [133]. Also, several groups have studied the cytotoxicity of various coated iron-oxide NPs [134–136]. Additionally, binding polymers such as poly (4-vinylpyridine) (PVP) used in antibacterial nanocomplexes are able to reduce the cytotoxicity of the nanostructures [137, 138].

5 Recyclability and retrieval of MNPs

Graphene oxide (GO) nanosheets have appeared as a promising platform to support Fe_3O_4 NPs that can provide them with facilitated separation and recyclability. In this approach, a stable GO-based nanocomplex is formed when the negatively charged GO is electrostatically attracted to a positively charged polymer such as *N*-alkylated PVP (NPVP) [84], polyethylenimine [139] or polystyrene [140]. That is when polymer-coated MNPs are introduced to GO nanosheets [141] forming a recyclable GO-based magnetic nanohybrid.

It is suggested that the observed reduction (though not significant) of the bactericidal activity in $Co_{0.3}Zn_{0.7}Fe_2O_4$/*Ocimum basilicum* seed's mucilage (OBM)/AgNPs could be due to an adsorption of proteins and nucleic acids released from withered bacterial cells on the surface of Ag ions [86]. $NiFe_2O_4$@ poly acrylonitrile-co-maleic anhydride (PAMA)@Ag–TiO_2 NPs were examined in a dynamic shaking flask method and were found to have a declined antibacterial effect against both *S. aureus* and *E. coli* by 30% after five cycles of application [142]. The most probable reason for this observation is attributed to the covered surface of NPs by dead bacterial cells [143].

6 Characterisation techniques of antibacterial MNPs

To reveal the antibacterial properties of nanomaterials, it is essential to examine them in two different aspects. An antibacterial nanomaterial primarily requires a comprehensive antibacterial characterisation, where its biologic response in the proximity of Gram-positive and Gram-negative bacteria is properly investigated. Coupled with its antibacterial performance, the chemical and physical natures of a nanomaterial must be thoroughly inspected so that its intrinsic traits such as morphology and elemental composition are known. This may significantly contribute to an understanding of interactions between nanomaterials and their target biosystem and would optimistically result in the development of more efficient antibacterial agents.

6.1 Antibacterial tests

An essential factor in developing new generation antimicrobial agents is to have a clear understanding of their impact on microbial cell viability. Traditionally, a variety of techniques have emerged to quantitatively demonstrate the antibacterial performance of medicines *in vitro*. In this section, a brief overview of selected common assays in the analysis of antibacterial effects of NPs is presented.

6.1.1 3-4,5-Dimethylthiazol-2-yl-2,5-diphenyltetrazolium bromide: In search of an assay for a quantitative evaluation of mammalian cell viability and proliferation, Mosmann [144] introduced a colorimetric method using MTT, a water-soluble tetrazolium salt, which provides the opportunity of detecting living cells, but not dead cells. A multiwell scanning spectrophotometer is then used to read the results with high precision. Rapidity and precision, along with a lack of radioisotope employment, are considered as the main advantages of this technique. Nowadays, MTT lies among the most common assays based on tetrazolium salts. In this method, the mitochondrial dehydrogenases of viable cells are mainly able to reduce the yellowish MTT to a purple insoluble formazan product [145–147].

6.1.2 Disc diffusion: This method is principally conducted by using a previously inoculated agar with a test microbe, where an antimicrobial containing disc is placed on it to produce an antimicrobial concentration radial gradient by uptaking moisture [148]. After proper incubation time, a clear zone of inhibition is formed around the disc if the examined substance is able to inhibit the bacterial growth. Thus, the susceptibility of microbial species to certain antimicrobials is displayed as the diameter of the inhibition zone.

Disc diffusion method has revealed that $NiFe_2O_4$@PAMA@Ag–TiO_2 NPs demonstrate a maximum antibacterial activity in comparison with $NiFe_2O_4$@Ag and bare AgNPs and create a zone of inhibition twice greater than that of AgNPs [142]. Also, the produced zone of inhibition by $Co_{0.3}Zn_{0.7}Fe_2O_4$/OBM/AgNPs has proved to be larger than that of AgNPs, which is presumably due to stabilisation of AgNPs on magnetic cores facilitated by the OBM layer. The results of antibacterial disc diffusion tests of Fe_3O_4@APTES–ethylenediaminetetraacetic acid (EDTA)@AgNPs confirmed that Ag deposition on the surface of Fe_3O_4@APTES–EDTA NPs enhanced their antibacterial performance [72].

6.1.3 Minimum inhibitory concentration: Minimum inhibitory concentration (MIC) is, by definition, the lowest concentration of an antimicrobial agent that, under certain test conditions, will inhibit the visible growth of the investigated microorganism [149]. This experiment is commonly considered as an essential assay in performance determination of new antimicrobials *in vitro*.

In case of Fe_3O_4@C@MgO and Fe_3O_4@C@MgO–Cu disinfectants, if the concentration of the NPs is cut down to a value less than MIC, test microbial strains of *S. aureus* and *E. coli* grow enough to produce a turbid suspension [85]. It is also observed that the same concentration of Fe_3O_4@C@MgO-Cu NPs (312.5 mg l^{-1}), which shows a 99% bactericidal effectiveness in shaking flask inactivation experiments, is only able to inhibit the strain growth in MIC experiments. The reason is attributed to the medium where the inactivation tests are performed, i.e. a normal saline solution, while in MIC tests the adopted nutrient broth medium may protect the microbial strains and hinder bactericidal effects [85].

6.1.4 Minimum bactericidal concentration: Minimum bactericidal concentration (MBC) test is typically performed in conjunction with MIC procedure to determine the minimum lethal concentration of an assayed antimicrobial agent to target bacterial species. The MBC value is taken as the lowest concentration of an antibacterial agent that diminishes the viability of bacterial strains by at least 99.9% [116].

In a recent study [150], MBC assays of $CuCr_xFe_{2-x}O_4$ samples were performed on the examined MIC plates with no growth, where a normal saline solution was added onto the plates before transferring them to fresh Mueller-Hinton Agar plates for a 24 h incubation. The MBCs were then recorded as the minimum concentration of NPs at which no bacterial growth is observed. Similarly, in an investigation of the antibacterial performance of $NiFe_2O_4$@TEOS–TPS@AgNPs [151], diluted NP solutions were added to the solutions of target broth bacterial inocula to undergo an incubation at 37°C for 24 h. The most diluted solution with no observable bacterial growth indicated the MIC. The diluted sample tubes were next transferred to nutrient agar plates to determine MBC values after another 24 h of incubation. That is when no observable bacterial growth is detected on the nutrient agar [152].

6.1.5 Flow cytometry: Flow cytometry technology has shed light on the analysis of physical and chemical properties of cell suspensions as they pass through laser radiation. This technique provides the opportunity to differentiate cells in terms of their size and density [153]. DNA intercalating dyes can be used in this method to determine cell apoptosis rates. DNA fragmentation is a characteristic feature of apoptotic cells, whereby a fluorochrome such as a propidium iodide (PI) is able to label DNA content in a flow cytometric assay [154].

The antibacterial properties of a wide range of MNPs have been investigated using flow cytometry method [83, 155–157]. Cellular uptake of silica-coated SPIONs was determined by inspecting an incorporated fluorescence intensity using a flow cytometry assay [158]. In this paper, Lu *et al.* showed that the cellular uptake of these NPs in human mesenchymal stem cells is time and dose dependent.

6.1.6 Live/dead fluorescent assay: In this technique, Syto9, a green fluorescent nucleic acid dye, is used to stain the healthy membrane of viable bacterial cells with intact membranes, producing a green fluorescence response. On the other hand, a red fluorescent nucleic acid dye named PI as another component of the kit is able to stain dead bacteria having deformed membranes which lead to an emission response in the red region [115, 159].

The antibacterial activity of Fe_3O_4-polydopamine (PDA)-AgNPs against *E. coli* was analysed using LIVE/DEAD BacLight bacterial viability kit [160], where strong green signals were observed in the absence of these NPs. In the presence of Fe_3O_4–PDA–AgNPs, tested bacteria presented red fluorescent signals, which indicated that most of the bacterial cells had been killed. The bacterial viabilities of *E. coli* and *S. aureus* were examined in the presence of Fe_3O_4–TiO_2 nanosheets (TNS) in a fluorescent-based cell live/dead test [161] and it was revealed that Fe_3O_4-TNS system inactivated both bacterial species. Similarly, the results of the live/dead assay on the antibacterial effects of Fe_3O_4 and Fe_2O_3 NPs on *S. aureus* cells revealed that the ratio of live/dead *S. aureus* was significantly decreased in the samples containing Fe_3O_4 and Fe_2O_3 NPs [162].

6.1.7 ROS determination test: A fluorescent dye assay using 2,7-dichlorodihydro-fluoresceindiacetate diacetate (DCFH-DA) has been employed to inspect the quantitative intracellular levels of ROS [121, 163]. In this method, DCFH-DA, which is a non-fluorescent dye and is able to readily permeate through the cell membrane, is hydrolysed to DCFH while in the intracellular space. The presence of ROS would turn DCFH into green fluorescent 2-7-dichlorofluorescein, a lipid-impermeable compound. The fluorescent response can then be captured using a confocal microscope for further analysis.

6.2 Magnetic response of MNPs

In probing the magnetic character of NPs, the precision provided by superconducting quantum interference devices has made them extensively popular tools among researchers [30, 51, 73, 164]. They are commonly integrated into magnetic properties measurement systems to conduct zero-field-cooled (FC) and FC magnetic susceptibility measurements [51]. Analogously, vibrating sample magnetometers are employed to study the magnetic character of NP samples.

Incorporation of non-magnetic layers on the surface of core magnetic materials often results in a considerable decline in their magnetic response (see Table 1 for the table of results).

6.3 Microscopy techniques

6.3.1 Atomic force microscopy: Individual-cell level investigation of biological processes provides a highly valuable opportunity of studying multiple biological properties of single cells that cannot be assessed by techniques that provide averaged information of large ensembles of molecules in many cells (e.g. X-ray crystallography and radioimmunoassay). Introduction of atomic force microscopy (AFM) has facilitated the nanoscale study of functional components in single living cells. In comparison to commonly used microscopy techniques in the field of NP science, along with providing a favourably high spatial resolution, AFM benefits from distinguishing advantages. For instance, optical microscopes are unable to visualise the structure of nano-sized cellular components, and electron microscopy techniques require dried and fixed cells. Observation of living cells in an aqueous environment is an appreciable asset of AFM, which brings dynamic biological responses of cells into a distinguished dimension of understanding. Also, AFM has made it possible to simultaneously obtain various measurement data on biological systems including their morphology, elasticity, adhesion, deformation and energy dissipation [165].

6.3.2 Scanning electron microscopy (SEM) and field emission SEM: SEM and field emission SEM (FESEM) techniques lie among the most versatile electron microscopy techniques in the characterisation of antimicrobial NPs. In conjunction with other characterisation techniques such as transmission electron microscopy (TEM), they can readily provide primary information on various features of NP samples including their shape, aggregation state, core–shell structure and size.

Conventional SEM benefits from several advantages when implemented for antimicrobial samples including its ability to be used for specimens with a wide variety of sizes from centimetre-sized cases to smaller scales. Visual information about material surface and its morphology is conventionally obtained using SEM. However, one major drawback of this technique is that samples must be dehydrated before introducing to the vacuum chamber of SEM devices. In the case of biological specimens, dehydration may disrupt their natural morphological characteristics as they undergo cellular shrinkage. Moreover, non-conductive specimens are difficult to scan in SEM instruments and conductive coatings such as Au on the surface of specimens are necessary in their sample preparation step.

In contrast to SEM mechanism of operation which uses a thermionic emission method, FESEM takes advantage of a field emission source often termed as a cold cathode field emitter, to make it a technique with one of the highest resolutions among microscopy methods. Along with presenting extra magnification in micrographs, FESEM devices can be set on a variety of scan modes including scanning TEM, which has been adopted in combination with an elemental mapping to detect metal NPs within the cellular zone of bacteria [157, 166].

6.3.3 Transmission electron microscopy: TEM is one of the most popular methods to obtain high-resolution (HR) visual details of samples in nanometre scales. This technique is capable of presenting elaborate visualisations of NPs, enabling us to attain

highly valuable information about size, shape, structure and crystalline parameters of nanoscale specimens.

For the electrons to pass through, the TEM target must be very thin, a preparation step which makes bulk samples difficult to probe.

6.3.4 Optical microscopy: The pioneering approaches to study the nature of microorganisms, which essentially facilitated the discovery of new species, involved extensive use of optical microscopes. HR optical imaging is now possible, thanks to advanced optics and digital imagery.

In the field of antimicrobial NPs, a rapid examination of microbial variations and interactions can be conducted in situ using optical microscopes. The optical diffraction limit of visible light would not ordinarily allow nanometre observations in optical microscopy; however, development of near-field scanning optical microscopy technique exceptionally provides axial and lateral resolutions of ∼20–50 and ∼5–10 nm, respectively [167].

6.4 Spectroscopy techniques

At both the fundamental and technological levels of research on nanomaterials, there is a strong incentive for innovative methods of characterisation to better understand and face nanomaterial challenges. Over recent years, major technological advances have taken place in certain branches of nanomaterial characterisation methods such as spectroscopy techniques, which have broadened horizons of nanomaterial examinations [168].

6.4.1 Raman spectroscopy: Raman spectra can confirm the formation of certain material phases in NP samples [65]. Confocal microprobe Raman systems are commonly used for obtaining conventional room-temperature Raman spectra [82]. Metal-oxygen vibrational modes can be characterised using Raman spectroscopy. In the Raman spectrum of $ZnFe_2O_4$ NPs, it is illustrated that the mode at 643 cm^{-1} corresponds to the motion of oxygen in tetrahedral sites (AO_4), while the observed lower-frequency modes are attributed to the oxygen motion in octahedral sites (BO_6) [169]. In another study, it is found that the sharp and intense Raman peak at 438 cm^{-1}, which indicates a highly crystalline sample with low intrinsic oxygen defects, is a characteristic of E_2(high) wurtzite lattice in Ag-decorated $ZnFe_2O_4$-dispersed ZnO nanoflakes [170]. In these composite nanoflakes, the small peaks at 382 and 574/582 cm^{-1} are found to represent the A_1(TO) and E_1(LO) modes, respectively, and the broad asymmetric peak at 1146/1150 cm^{-1} corresponds to a second-order (2LO) Raman mode. Raman active modes of both Co_3O_4 and α-Fe_2O_3 are detected in α-Fe_2O_3/Co_3O_4 nanocomposite system [82], where vibrations of A_1g octahedral sites of Co_3O_4 are represented by a peak at 679 cm^{-1} and coupled vibrations of tetrahedral and octahedral sites are characterised by F_2g and E_g modes. In case of haematite phase (α-Fe_2O_3), the Fe–O vibrational stretching modes are characterised by peaks at 226.8, 292.5, 400, 486.5 and 600 cm^{-1} [95].

6.4.2 X-ray photoelectron spectroscopy: X-ray photoelectron spectroscopy (XPS) can be adopted as a tool to verify the formation of certain materials. It is a surface technique that examines surface layers which are generally more oxidised and is also capable of assessing the chemical state of the components [171].

XPS peaks at 723 and 710 eV correspond to the energies of $2p_{3/2}$ and $2p_{1/2}$ spin-orbit components in pure Fe_3O_4 NPs [30]. By coating silica on these NPs, aside from characteristic peak of silica at 103 eV, the intensity of Fe_3O_4 peaks is decreased and on the emergence of a peak at 399 eV, functionalisation of amine ($–NH_2$) on the surface of Fe_3O_4–SiO_2 core–shell is verified.

6.4.3 Ultraviolet–visible (UV–vis) spectrophotometry: The optical absorption rate of suspensions plays an important role in the characterisation of NPs which can be obtained using UV–vis spectrophotometry technique. Moreover, this method is essentially used to detect surface plasmon resonance peak of metal NPs [121].

In quantitative studies adopting UV–vis assays, it is found that absorption rate can be interpreted as the amount of unabsorbed drug in magnetic nanocarrier samples [172]. In another study [38], UV–vis diffuse reflection spectroscopy was used to measure the energy band gap of conventionally synthesised $CoFe_2O_4$ NPs in the visible region which was determined to be 2.09 eV.

6.4.4 Infrared (IR) and Fourier transform IR (FTIR) spectroscopy: A comprehensive review of qualitative and quantitative near-IR spectroscopies have been provided by Roggo *et al.* [173]. FTIR spectroscopy is mainly adopted in traditional nanoscience for investigating the existing molecules and surface chemical groups of samples [51], verifying various formed chemical bonds [36] and confirming drug loading onto nanocarriers [172].

A recent study by Yu *et al.* [174] involved FTIR investigations on Fe_3O_4@PDA nanocomposites, which exhibited an absorption band at 1284 cm^{-1}, which is a typical band of primary amine vibration. The Fe–O bonds in FTIR spectra are reported to exhibit a strong peak at about 585 cm^{-1} [36].

6.4.5 Energy dispersive X-ray spectroscopy: Energy dispersive X-ray spectroscopy (EDS) plays an important role in the characterisation of nanomaterials. It is typically capable of probing the specimens up to a few micrometres depth. In a novel magnetic barium (Ba) phosphate nanoflake material synthesised by Song *et al.* [35], the element mapping results of EDS scans in these nanoflakes containing embedded iron-oxide NPs have confirmed the uniform distribution of Fe, Ba and phosphorous in the composite. Also, the elemental constitution of GO-Ag and GO-Fe_3O_4@NPVP-AgNPs analysed by EDS revealed that carbon, oxygen and Ag were the principal elements present in them [84]. In Ag/$CuFe_2O_4$ MNPs, the atomic fractions of Fe, O, Cu and Ag were obtained by EDS results as 35.29, 54.3, 4.19 and 6.21%, respectively, where an obvious signal of Ag element verifies that AgNPs were successfully doped on the $CuFe_2O_4$ [33].

6.5 Other conventional techniques

6.5.1 Contact angle (CA) and surface free energy: Through inspecting quantitative hydrophobicity or hydrophilicity of material surfaces, an evaluation of their surface free energy (SFE) can be achieved using CA measurements. It is observed that the SFE of material surfaces can be viewed as a key parameter in their antimicrobial activity, as the ability of microorganisms to contact and adhere to surfaces is a deciding factor of their viability therein.

CA is basically defined as the equilibrium angle, where the drop of probe liquid touches the underneath solid surface. As described by Young's relation, the equilibrium CA on flat homogeneous surfaces is expressed by $\gamma \cos \theta_E = \gamma_{SV} - \gamma_{SL}$, where γ, γ_{SL} and γ_{SV} denote surface tensions at the liquid–vapour, solid–liquid and solid–vapour interfaces, respectively [175]. This equation does not favourably apply to polymers due to their non-ideal surfaces made of liquid-penetrable matrices. An important physical phenomenon associated with CA measurement is CA hysteresis, which is intuitively understood by looking at the asymmetric droplet shapes sitting on vertical surfaces. In other words, the equilibrium CA can take values of an angle range, which is called the CA hysteresis [176].

Surface parameters of NPs such as wettability can be studied by CA measurements. In an iron-oxide-containing nanocomplex, it is observed that coating with cysteine and lawsone decreases the CA on stainless steel, meaning that the wettability of these iron-oxide NPs is greatly increased on such coatings [177]. These MNPs are suggested to be effective in corrosion inhibition applications. By observing the decrease in CA values of water droplets on the incorporation of AgNPs into chitosan–starch-based films, it is concluded that water is more accessible to the surface of the AgNPs loaded films [178].

In a recent study, the effect of iron-oxide NPs over biofilm formation on different biomaterial surfaces has revealed that combination of polymer brush coating and iron-oxide NPs leads to a significant reduction in bacterial adhesion on pluronic-coated surfaces [179]. In this paper, using sessile drop technique, wettability of biomaterial surfaces was determined by water CA measurements, which exhibited a significant reduction in bacterial adhesion to polyethylene oxide (PEO) brushed surfaces. Results indicate a significant reduction in biofilm growth due to the antibacterial effect of PEO-brushed coatings combined with iron-oxide NPs.

6.5.2 X-ray diffraction: X-ray diffraction (XRD) method is generally based on the principle that each crystalline system can be identified by its characteristic diffraction pattern. The periodic nature of a crystalline lattice allows scattering of X-ray radiation based on Bragg's law. XRD is traditionally used for characterisation of nanocrystalline samples and verifying their chemical composition [33, 45, 115]. Phase identification capability of the XRD technique is traditionally employed to inspect phase characteristics and parameters before and after modifications made to NPs.

6.5.3 Dynamic light scattering: In terms of the introduced applications to MNPs, particle size distribution stands out as one of the most important parameters as many of chemical and physical properties of MNPs strongly depend on it. Dynamic light scattering (DLS) has been one of the most extensively employed techniques in determining the particle size distribution of NP suspensions in a facile manner [64, 180]. However, interpretation of DLS data may suffer from a lack of unevaluated sample and measurement parameters including the concentration of suspensions, colloidal stability and shape anisotropy of particles that would partly affect the precision of results.

In a DLS measurement procedure, a suspension of target particles is exposed to a light beam which is scattered as a result of impinging on dispersed particles. During the measurement time span, the Brownian motion of suspended particles alters the intensity of the incident light. The variation of light intensity essentially contains valuable information about the diffusion coefficient of particles. The diffusion coefficient of particles can be employed to calculate their hydrodynamic radius, R_H, by taking account of solvent viscosity [181]. The hydrodynamic radius belongs to a sphere with the same diffusion coefficient as the assayed particles. DLS results are highly sensitive to particle aggregation and are considered as an appealing evaluation of colloidal stability.

Particle size measurements performed using the DLS method have been reported to hold dependence on pH levels of suspensions. In a DLS measurement of GO-Fe_3O_4@NPVP-Ag composite NPs in aqueous environment, it is found that the size of particles exhibits a pH-responsive behaviour as their average size at low pH levels is about 700 nm, whereas it is decreased to <300 nm at higher pH values [84].

6.5.4 Zeta potential: Zeta potential of NPs is interpreted as a measure of their colloidal stability, where high zeta potential values of small enough dispersed particles would resist their propensity to aggregate. By applying an electric field across the dispersion, the zeta potential of dispersed particles is measured by inspecting their electrophoretic mobility using a light scattering method. It is established that NP dispersions could be considered stable if their zeta potential magnitude exceeds 30 mV [182].

Maintaining a positive surface charge essentially allows NPs to entrap bacteria possessing negatively charged surfaces [30]. It is demonstrated that chitosan coating of iron-oxide NPs can successfully alter their negative zeta potential value from −32.2 to +36.3 mV, yet improving their antimicrobial effects [115]. Similarly, in a report by Li *et al.* [84], GO-Fe_3O_4@NPVP-Ag antibacterial nanocomposites were able to reverse their negative surface charge value in physiological pH to a positive value in acidic condition.

Among antibacterial magnetic hybrid nanostructures such as Fe_3O_4/p-aminobenzoic acid MNPs coated with bee pollen extracts (BPE) [183], it is found that natural compounds (e.g. BPE) may contribute to avoid aggregation of nanosystems by enhancing their zeta potential values.

7 Potential way and challenges of antibacterial MNPs

The potential antibacterial performance of MNPs was demonstrated with various sizes and shapes. Conjugated MNPs with organic or inorganic counterparts were also investigated together with their antibacterial effects. Low cost of such MNPs makes them reasonable candidates for clinical applications. MNPs may be viewed as excellent tools that can feasibly target specific sites that are not effectively reached by other biomedical agents. However, the limited available knowledge of their metabolic effects, removal and toxicity is considered as a drawback in biomedical applications of MNPs.

8 Conclusion

The investigation of MNPs has shown that they offer a high potential for therapeutic applications specifically as antibacterial nanoagents. While major global health issues such as multi-drug-resistant bacteria continue to threaten lives, the advantages of MNPs including their favourable response to magnetic fields, large surface area, recyclability and biocompatibility allow for their use in a wide range of applications in nanoscience and nanomedicine. Aside from providing biocompatibility for MNPs, surface coating technique has been thought of as a key factor in optimising MNPs for impressive applications such as their effects against bacteria. Incorporation of biocompatible polymer layers is an excellent way to stop MNPs from aggregation and provide a linkage to include other NPs in their structure.

Various characterisation techniques have been developed over the past decades to probe multiple properties of nanostructured materials. Many assays present qualitative and quantitative analyses of antibacterial effects for synthesised NPs. Combined with microscopic and spectroscopic methods, these assays establish a comprehensive knowledge regarding the physical and chemical properties of magnetic antibacterial NPs. Although promising success has been achieved in the antimicrobial performance of MNPs *in vitro*, it is expected to find extraordinary *in vivo* applications of these NPs by expanding the understanding of biological and physiochemical properties of MNPs in future research.

9 References

[1] World Health Organization: '*Global tuberculosis report 2018*' (World Health Organization, Geneva, Switzerland, 2018)

[2] Mukherjee, S.: 'Emerging infectious diseases: epidemiological perspective', *Indian J. Dermatol.*, 2017, **62**, (5), pp. 459–467

[3] 'Swine influenza – WHO'. Available at https://www.who.int/mediacentre/news/statements/2009/h1n1_20090425/en/, accessed 25 April 2009

[4] Kaviyarasu, K., Maria Magdalane, C., Kanimozhi, K., *et al.*: 'Elucidation of photocatalysis, photoluminescence and antibacterial studies of ZnO thin films by spin coating method', *J. Photochem. Photobiol. B, Biol.*, 2017, **173**, pp. 466–475

[5] Hossan, M.S., Jindal, H., Maisha, S., *et al.*: 'Antibacterial effects of 18 medicinal plants used by the *Khyang* tribe in Bangladesh', *Pharm. Biol.*, 2018, **56**, (1), pp. 201–208

[6] Slavin, Y.N., Asnis, J., Häfeli, U.O., *et al.*: 'Metal nanoparticles: understanding the mechanisms behind antibacterial activity', *J. Nanobiotechnol.*, 2017, **15**, (1), p. 65

[7] Rodrigues, G.R., López-Abarrategui, C., de la Serna Gómez, I., *et al.*: 'Antimicrobial magnetic nanoparticles based-therapies for controlling infectious diseases', *Int. J. Pharm.*, 2019, **555**, pp. 356–367

[8] Anselmo, A.C., Mitragotri, S.: 'A review of clinical translation of inorganic nanoparticles', *AAPS J.*, 2015, **17**, (5), pp. 1041–1054

[9] Allafchian, A.R., Jalali, S.A.H., Aghaei, F., *et al.*: 'Green synthesis of silver nanoparticles using *Glaucium corniculatum* (L.) Curtis extract and evaluation of its antibacterial activity', *IET Nanobiotechnol.*, 2018, **12**, (5), pp. 574–578

[10] Zandpour, F., Allafchian, A.R., Vahabi, M.R., *et al.*: 'Green synthesis of silver nanoparticles with the arial part of *Dorema ammoniacum* D. extract by antimicrobial analysis', *IET Nanobiotechnol.*, 2018, **12**, (4), pp. 491–495

[11] Allafchian, A.R., Farhang, H.R., Jalali, S.A.H., *et al.*: '*Gundelia tournefortii* L.: a natural source for the green synthesis of silver nanoparticles', *IET Nanobiotechnol.*, 2017, **11**, (7), pp. 815–820

[12] Li, Z., Barnes, J.C., Bosoy, A., *et al.*: 'Mesoporous silica nanoparticles in biomedical applications', *Chem. Soc. Rev.*, 2012, **41**, (7), pp. 2590–2605

[13] Connor, D.M., Broome, A.-M.: 'Chapter seven – gold nanoparticles for the delivery of cancer therapeutics', in Broome, A.-M. (Ed.): '*Cancer nanotechnology*' (Academic Press, USA, 2018), pp. 163–184

[14] Vallabani, N.V.S., Singh, S.: 'Recent advances and future prospects of iron oxide nanoparticles in biomedicine and diagnostics', *3 Biotech*, 2018, **8**, (6), p. 279

[15] Burns, A., Self, W.T.: '11 – antioxidant inorganic nanoparticles and their potential applications in biomedicine', in Ciofani, G. (Ed.): '*Smart nanoparticles for biomedicine*' (Elsevier, Amsterdam, The Netherlands, 2018), pp. 159–169

[16] Ikeda, Y., Shoji, K., Feliciano, C.P., *et al.*: 'Antioxidative nanoparticles significantly enhance therapeutic efficacy of an antibacterial therapy against *Listeria monocytogenes* infection', *Mol. Pharm.*, 2018, **15**, (3), pp. 1126–1132

[17] Franci, G., Falanga, A., Galdiero, S., *et al.*: 'Silver nanoparticles as potential antibacterial agents', *Molecules*, 2015, **20**, (5), pp. 8856–8874

[18] Hainfeld, J.F., Slatkin, D.N., Smilowitz, H.M.: 'The use of gold nanoparticles to enhance radiotherapy in mice', *Phys. Med. Biol.*, 2004, **49**, (18), p. 309

[19] Elzoghby, A.O., Freag, M.S., Elkhodairy, K.A.: 'Biopolymeric nanoparticles for targeted drug delivery to brain tumors', in Prashant, K., Gupta, U. (Eds.): '*Nanotechnology-based targeted drug delivery systems for brain tumors*' (Elsevier, USA, 2018), pp. 169–190

[20] Agrahari, V.: 'The exciting potential of nanotherapy in brain-tumor targeted drug delivery approaches', *Neural Regen. Res.*, 2017, **12**, (2), pp. 197–200

[21] Bischoff, F.Z., Mathieu, K.B., Pang, L., *et al.*: 'Detection and measurement of HER2+ breast cancer cells using tumor-targeted iron oxide nanoparticles and magnetic relaxometry', *J. Clin. Oncol.*, 2018, **36**, (15_suppl), p. e13019

[22] Park, J.H., von Maltzahn, G., Zhang, L., *et al.*: 'Magnetic iron oxide nanoworms for tumor targeting and imaging', *Adv. Mater.*, 2008, **20**, (9), pp. 1630–1635

[23] Li, R., He, Y., Zhang, S., *et al.*: 'Cell membrane-based nanoparticles: a new biomimetic platform for tumor diagnosis and treatment', *Acta Pharm. Sin. B*, 2018, **8**, (1), pp. 14–22

[24] Huber, D.L.: 'Synthesis, properties, and applications of iron nanoparticles', *Small*, 2005, **1**, (5), pp. 482–501

[25] Wierzbinski, K.R., Szymanski, T., Rozwadowska, N., *et al.*: 'Potential use of superparamagnetic iron oxide nanoparticles for *in vitro* and *in vivo* bioimaging of human myoblasts', *Sci. Rep.*, 2018, **8**, (1), p. 3682

[26] Fingerhut, A.G., Alksne, J.F.: 'Thrombosis of intracranial aneurysms. an experimental approach utilizing magnetically controlled iron particles', *Radiology*, 1966, **86**, (2), pp. 342–343

[27] Nigam, S., Bahadur, D.: 'Doxorubicin-loaded dendritic-Fe_3O_4 supramolecular nanoparticles for magnetic drug targeting and tumor regression in spheroid murine melanoma model', *Nanomed. Nanotechnol. Biol. Med.*, 2018, **14**, (3), pp. 759–768

[28] de Almeida Roger, J., Magro, M., Spagnolo, S., *et al.*: 'Antimicrobial and magnetically removable tannic acid nanocarrier: a processing aid for *Listeria monocytogenes* treatment for food industry applications', *Food Chem.*, 2018, **267**, pp. 430–436

[29] Stoimenov, P.K., Klinger, R.L., Marchin, G.L., *et al.*: 'Metal oxide nanoparticles as bactericidal agents', *Langmuir*, 2002, **18**, (17), pp. 6679–6686

[30] Chaurasia, A.K., Thorat, N.D., Tandon, A., *et al.*: 'Coupling of radiofrequency with magnetic nanoparticles treatment as an alternative physical antibacterial strategy against multiple drug resistant bacteria', *Sci. Rep.*, 2016, **6**, p. 33662

[31] Rahman, M.A., Radhakrishnan, R., Gopalakrishnan, R.: 'Structural, optical, magnetic and antibacterial properties of Nd doped NiO nanoparticles prepared by co-precipitation method', *J. Alloys Compd.*, 2018, **742**, pp. 421–429

[32] Bilas, R., Sriram, K., Maheswari, P.U., *et al.*: 'Highly biocompatible chitosan with super paramagnetic calcium ferrite ($CaFe_2O_4$) nanoparticle for the release of ampicillin', *Int. J. Biol. Macromol.*, 2017, **97**, pp. 513–525

[33] Atacan, K., Özacar, M., Özacar, M.: 'Investigation of antibacterial properties of novel papain immobilized on tannic acid modified Ag/$CuFe_2O_4$ magnetic nanoparticles', *Int. J. Biol. Macromol.*, 2018, **109**, pp. 720–731

[34] Ehi-Eromosele, C.O., Olugbuyiro, J., Edobor-Osoh, A., *et al.*: 'Magneto-structural and antimicrobial properties of sodium doped lanthanum manganite magnetic nanoparticles for biomedical applications: influence of silica coating', *J. Biomimetics Biomater. Biomed. Eng.*, 2018, **37**, pp. 117–127

[35] Song, J., Zhang, F., Huang, Y., *et al.*: 'Highly efficient bacterial removal and disinfection by magnetic barium phosphate nanoflakes with embedded iron oxide nanoparticles', *Environ. Sci. Nano*, 2018, **5**, (6), pp. 1341–1349

[36] Rajabi, S., Sohrabnezhad, S.: 'Fabrication and characteristic of Fe_3O_4@MOR@CuO core–shell for investigation antibacterial properties', *J. Fluorine Chem.*, 2018, **206**, pp. 36–42

[37] El-Liethy, M.A., Elwakeel, K.Z., Ahmed, M.S.: 'Comparison study of Ag (I) and Au (III) loaded on magnetic thiourea-formaldehyde as disinfectants for water pathogenic microorganism's deactivation', *J. Environ. Chem. Eng.*, 2018, **6**, (4), pp. 4380–4390

[38] Kombaiah, K., Vijaya, J.J., Kennedy, L.J., *et al.*: 'Okra extract-assisted green synthesis of $CoFe_2O_4$ nanoparticles and their optical, magnetic, and antimicrobial properties', *Mater. Chem. Phys.*, 2018, **204**, pp. 410–419

[39] Ezhilarasi, A.A., Vijaya, J.J., Kaviyarasu, K., *et al.*: 'Green synthesis of NiO nanoparticles using *Aegle marmelos* leaf extract for the evaluation of in-vitro cytotoxicity, antibacterial and photocatalytic properties', *J. Photochem. Photobiol. B, Biol.*, 2018, **180**, pp. 39–50

[40] Hariani, P.L., Desnelli, D., Fatma, F., *et al.*: 'Synthesis and characterization of Fe_3O_4 nanoparticles modified with polyethylene glycol as antibacterial material', *J. Pure Appl. Chem. Res.*, 2018, **7**, (2), p. 122

[41] El-Bassuony, A.A., Abdelsalam, H.: 'Attractive improvement in structural, magnetic, optical, and antimicrobial activity of silver delafossite by Fe/Cr doping', *J. Supercond. Novel Magn.*, 2018, **31**, (11), pp. 1–13

[42] Bomila, R., Srinivasan, S., Gunasekaran, S., *et al.*: 'Enhanced photocatalytic degradation of methylene blue dye, opto-magnetic and antibacterial behaviour of pure and La-doped ZnO nanoparticles', *J. Supercond. Novel Magn.*, 2018, **31**, (3), pp. 855–864

[43] Ahmadi, F., Rahimi-Nasrabadi, M., Daneshmehr, M., *et al.*: 'Synthesis, characterization, and investigation of magnetic, photocatalytic and antibacterial properties of $TbVO_4$ nanoparticles', *J. Mater. Sci., Mater. Electron.*, 2017, **28**, (19), pp. 14362–14368

[44] Rana, S.B., Singh, R., Arya, S.: 'Structural, optical, magnetic and antibacterial study of pure and cobalt doped ZnO nanoparticles', *J. Mater. Sci., Mater. Electron.*, 2017, **28**, (3), pp. 2660–2672

[45] Wei, W., Zhaohui, W., Taekyung, Y., *et al.*: 'Recent progress on magnetic iron oxide nanoparticles: synthesis, surface functional strategies and biomedical applications', *Sci. Technol. Adv. Mater.*, 2015, **16**, (2), p. 023501

[46] Elwakeel, K.Z., El-Liethy, M.A., Ahmed, M.S., *et al.*: 'Facile synthesis of magnetic disinfectant immobilized with silver ions for water pathogenic microorganism's deactivation', *Environ. Sci. Pollut. Res.*, 2018, **25**, (23), pp. 1–13

[47] Liu, Y., Zhang, K., Yin, X., *et al.*: 'Highly reusability surface loaded metal particles magnetic catalyst microspheres (MCM-MPs) for treatment of dye-contaminated water', *J. Magn. Magn. Mater.*, 2016, **403**, pp. 18–29

[48] Markiewicz, K.H., Misztalewska-Turkowicz, I., Niemirowicz, K., *et al.*: 'Carbamohydrazonothioate-based polymer-magnetic nanohybrids: fabrication, characterization and bactericidal properties', *Arab. J. Chem.*, 2016, in press

[49] Silva, S.M., Tavallaie, R., Sandiford, L., *et al.*: 'Gold coated magnetic nanoparticles: from preparation to surface modification for analytical and biomedical applications', *Chem. Commun.*, 2016, **52**, (48), pp. 7528–7540

[50] Santhoshkumar, A., Kavitha, H.P., Suresh, R.: 'Preparation, characterization and antibacterial activity of NiO nanoparticles', *Asian J. Chem.*, 2017, **29**, (2), pp. 239–241

[51] Peng, B., Zhang, X., Aarts, D.G., *et al.*: 'Superparamagnetic nickel colloidal nanocrystal clusters with antibacterial activity and bacteria binding ability', *Nat. Nanotechnol.*, 2018, **13**, (6), p. 478

[52] Wells, M.L., Potin, P., Craigie, J.S., *et al.*: 'Algae as nutritional and functional food sources: revisiting our understanding', *J. Appl. Phycol.*, 2017, **29**, (2), pp. 949–982

[53] Arokiyaraj, S., Saravanan, M., Udaya Prakash, N.K., *et al.*: 'Enhanced antibacterial activity of iron oxide magnetic nanoparticles treated with *Argemone mexicana* L. leaf extract: an in vitro study', *Mater. Res. Bull.*, 2013, **48**, (9), pp. 3323–3327

[54] Kekuda, T.P.: 'Antimicrobial, radical scavenging, and insecticidal activity of leaf and flower extracts of Couroupita guianensis Aubl', *Int. J. Green Pharm.*, 2017, **11**, (3), pp. 171–179

[55] Roumy, V., Gutierrez-Choquevilca, A.-L., Mesia, J.P.L., *et al.*: '*In vitro* antimicrobial activity of traditional plant used in mestizo shamanism from the Peruvian Amazon in case of infectious diseases', *Pharmacogn. Mag.*, 2015, **11**, (Suppl 4), p. S625

[56] Subramaniam, J., Murugan, K., Panneerselvam, C., *et al.*: 'Multipurpose effectiveness of Couroupita guianensis-synthesized gold nanoparticles: high antiplasmodial potential, field efficacy against malaria vectors and synergy with *Aplocheilus lineatus* predators', *Environ. Sci. Pollut. Res.*, 2016, **23**, (8), pp. 7543–7558

[57] Juvekar, M., Juvekar, A., Kulkarni, M., *et al.*: 'Phytochemical and pharmacological studies on the leaves of Couroupita guianensis Aubl', *Planta Medica* 2009, **75**, (9), p. PJ168

[58] Golkhatmi, F.M., Bahramian, B., Mamarabadi, M.: 'Application of surface modified nano ferrite nickel in catalytic reaction (epoxidation of alkenes) and investigation on its antibacterial and antifungal activities', *Mater. Sci. Eng., C*, 2017, **78**, pp. 1–11

[59] Beygi, H., Sajjadi, S.A.: 'Magnetic properties of crystalline nickel and low phosphorus amorphous $Ni_{1-x}P_x$ nanoparticles', *Mater. Chem. Phys.*, 2018, **204**, pp. 403–409

[60] Badnore, A.U., Salvi, M.A., Jadhav, N.L., *et al.*: 'Comparison and characterization of Fe_3O_4 nanoparticles synthesized by conventional magnetic stirring and sonochemical method', *Adv. Sci. Lett.*, 2018, **24**, (8), pp. 5681–5686

[61] Belaïd, S., Stanicki, D., Vander Elst, L., *et al.*: 'Influence of experimental parameters on iron oxide nanoparticle properties synthesized by thermal decomposition: size and nuclear magnetic resonance studies', *Nanotechnology*, 2018, **29**, (16), p. 165603

[62] Kastrinaki, G., Lorentzou, S., Karagiannakis, G., *et al.*: 'Parametric synthesis study of iron based nanoparticles via aerosol spray pyrolysis route', *J. Aerosol Sci.*, 2018, **115**, pp. 96–107

[63] Bunge, A., Porav, A.S., Borodi, G., *et al.*: 'Correlation between synthesis parameters and properties of magnetite clusters prepared by solvothermal polyol method', *J. Mater. Sci.*, 2019, **54**, (4), pp. 2853–2875

[64] Sathish Kumar, G., Logeshwaran, V., Sarathbabu, S., *et al.*: 'Green synthesis of magnetic Fe_3O_4 nanoparticles using Couroupita guianensis Aubl. fruit extract for their antibacterial and cytotoxicity activities', *Artif. Cells Nanomed. Biotechnol.*, 2018, **46**, (3), pp. 589–598

[65] Yew, Y.P., Shameli, K., Miyake, M., *et al.*: 'Green biosynthesis of superparamagnetic magnetite Fe_3O_4 nanoparticles and biomedical

applications in targeted anticancer drug delivery system: a review', *Arab. J. Chem.*, 2018, in press
[66] Bee, A., Massart, R., Neveu, S.: 'Synthesis of very fine maghemite particles', *J. Magn. Magn. Mater.*, 1995, **149**, (1–2), pp. 6–9
[67] Babes, L., Denizot, B.T., Tanguy, G., *et al.*: 'Synthesis of iron oxide nanoparticles used as MRI contrast agents: a parametric study', *J. Colloid Interface Sci.*, 1999, **212**, (2), pp. 474–482
[68] Bárcena, C., Sra, A.K., Gao, J.: 'Applications of magnetic nanoparticles in biomedicine', in Liu, J.P., Fullerton, E., Gutfleisch, O., *et al.* (Eds.): '*Nanoscale magnetic materials and applications*' (Springer, US, 2009), pp. 591–626
[69] Lutz, J.F., Stiller, S., Hoth, A., *et al.*: 'One-pot synthesis of PEGylated ultrasmall iron-oxide nanoparticles and their *in vivo* evaluation as magnetic resonance imaging contrast agents', *Biomacromolecules*, 2006, **7**, (11), pp. 3132–3138
[70] Guo, J., Chen, S., Liu, L., *et al.*: 'Adsorption of dye from wastewater using chitosan–CTAB modified bentonites', *J. Colloid Interface Sci.*, 2012, **382**, (1), pp. 61–66
[71] Abdelwahab, N., Morsy, E.: 'Synthesis and characterization of methyl pyrazolone functionalized magnetic chitosan composite for visible light photocatalytic degradation of methylene blue', *Int. J. Biol. Macromol.*, 2018, **108**, pp. 1035–1044
[72] Mirahmadi Zare, S., Allafchian, A., Jalali, S.: 'Core–shell fabrication of an extra-antimicrobial magnetic agent with synergistic effect of substrate ligand to increase the antimicrobial activity of Ag nanoclusters', *Environ. Prog. Sustain. Energy*, 2018, **38**, (1), pp. 237–245
[73] Mahmoudi, M., Serpooshan, V.: 'Silver-coated engineered magnetic nanoparticles are promising for the success in the fight against antibacterial resistance threat', *ACS Nano*, 2012, **6**, (3), pp. 2656–2664
[74] Schumacher, D., Helma, J., Schneider, A.F.L., *et al.*: 'Nanobodies: chemical functionalization strategies and intracellular applications', *Angew. Chem., Int. Ed.*, 2017, **57**, (9), pp. 2314–2333
[75] Yang, D.S., Jung, D.J., Choi, S.H.: 'One-step functionalization of multi-walled carbon nanotubes by radiation-induced graft polymerization and their application as enzyme-free biosensors', *Radiat. Phys. Chem.*, 2010, **79**, (4), pp. 434–440
[76] Hirschbiel, A.F., Schmidt, B.V., Krolla-Sidenstein, P., *et al.*: 'Photochemical design of stimuli-responsive nanoparticles prepared by supramolecular host–guest chemistry', *Macromolecules*, 2015, **48**, (13), pp. 4410–4420
[77] Su, N., Hu, X., Zhang, J., *et al.*: 'Plasma-induced synthesis of Pt nanoparticles supported on TiO_2 nanotubes for enhanced methanol electro-oxidation', *Appl. Surf. Sci.*, 2017, **399**, pp. 403–410
[78] Wang, L., Dong, L., Li, L., *et al.*: 'Fabrication of periodically micropatterned magnetite nanoparticles by laser-interference-controlled electrodeposition', *J. Mater. Sci.*, 2018, **53**, (5), pp. 3239–3249
[79] Francesko, A., Blandón, L., Vázquez, M., *et al.*: 'Enzymatic functionalization of cork surface with antimicrobial hybrid biopolymer/silver nanoparticles', *ACS Appl. Mater. Interfaces*, 2015, **7**, (18), pp. 9792–9799
[80] Wang, T., Ma, B., Jin, A., *et al.*: 'Facile loading of Ag nanoparticles onto magnetic microsphere by the aid of a tannic acid-metal polymer layer to synthesize magnetic disinfectant with high antibacterial activity', *J. Hazardous Mater.*, 2018, **342**, pp. 392–400
[81] Amanulla, A.M., Shahina, S.J., Sundaram, R., *et al.*: 'Antibacterial, magnetic, optical and humidity sensor studies of β-$CoMoO_4$-Co_3O_4 nanocomposites and its synthesis and characterization', *J. Photochem. Photobiol. B, Biol.*, 2018, **183**, pp. 233–241
[82] Bhushan, M., Kumar, Y., Periyasamy, L., *et al.*: 'Antibacterial applications of α-Fe_2O_3/Co_3O_4 nanocomposites and study of their structural, optical, magnetic and cytotoxic characteristics', *Appl. Nanosci.*, 2018, **8**, (1–2), pp. 137–153
[83] Kooti, M., Sedeh, A.N., Motamedi, H., *et al.*: 'Magnetic graphene oxide inlaid with silver nanoparticles as antibacterial and drug delivery composite', *Appl. Microbiol. Biotechnol.*, 2018, **102**, (8), pp. 3607–3621
[84] Li, Q., Yong, C., Cao, W., *et al.*: 'Fabrication of charge reversible graphene oxide-based nanocomposite with multiple antibacterial modes and magnetic recyclability', *J. Colloid Interface Sci.*, 2018, **511**, pp. 285–295
[85] Zhang, X., Wang, W., Zhang, Y., *et al.*: 'Loading Cu-doped magnesium oxide onto surface of magnetic nanoparticles to prepare magnetic disinfectant with enhanced antibacterial activity', *Colloids Surf. B, Biointerfaces*, 2018, **161**, pp. 433–441
[86] Allafchian, A., Jalali, S.A.H., Hosseini, F., *et al.*: '*Ocimum basilicum* mucilage as a new green polymer support for silver in magnetic nanocomposites: production and characterization', *J. Environ. Chem. Eng.*, 2017, **5**, (6), pp. 5912–5920
[87] Allafchian, A., Bahramian, H., Jalali, S.A.H., *et al.*: 'Synthesis, characterization and antibacterial effect of new magnetically core–shell nanocomposites', *J. Magn. Magn. Mater.*, 2015, **394**, pp. 318–324
[88] Jing, L., Xu, Y., Huang, S., *et al.*: 'Novel magnetic $CoFe_2O_4$/Ag/Ag_3VO_4 composites: highly efficient visible light photocatalytic and antibacterial activity', *Appl. Catal. B, Environ*, 2016, **199**, pp. 11–22
[89] Netzer, K., Jordakieva, G., Girard, A.M., *et al.*: 'Next-generation magnetic nanocomposites: cytotoxic and genotoxic effects of coated and uncoated ferric cobalt boron (FeCoB) nanoparticles *in vitro*', *Basic Clin. Pharmacol. Toxicol.*, 2018, **122**, (3), pp. 355–363
[90] Fu, P.P., Xia, Q., Hwang, H.-M., *et al.*: 'Mechanisms of nanotoxicity: generation of reactive oxygen species', *J. Food Drug Anal.*, 2014, **22**, (1), pp. 64–75
[91] Jose Ruben, M., Jose Luis, E., Alejandra, C., *et al.*: 'The bactericidal effect of silver nanoparticles', *Nanotechnology*, 2005, **16**, (10), p. 2346
[92] Auffan, M., Achouak, W., Rose, J., *et al.*: 'Relation between the redox state of iron-based nanoparticles and their cytotoxicity toward *Escherichia coli*', *Environ. Sci. Technol.*, 2008, **42**, (17), pp. 6730–6735
[93] Digigow, R.G., Dechézelles, J.-F., Dietsch, H., *et al.*: 'Preparation and characterization of functional silica hybrid magnetic nanoparticles', *J. Magn. Magn. Mater.*, 2014, **362**, pp. 72–79
[94] Kralj, S., Makovec, D., Čampelj, S., *et al.*: 'Producing ultra-thin silica coatings on iron-oxide nanoparticles to improve their surface reactivity', *J. Magn. Magn. Mater.*, 2010, **322**, (13), pp. 1847–1853
[95] Fazio, E., Santoro, M., Lentini, G., *et al.*: 'Iron oxide nanoparticles prepared by laser ablation: synthesis, structural properties and antimicrobial activity', *Colloids Surf. A, Physicochem. Eng. Aspects*, 2016, **490**, pp. 98–103
[96] Mitragotri, S., Lahann, J.: 'Physical approaches to biomaterial design', *Nature Mater.*, 2009, **8**, (1), p. 15
[97] Champion, J.A., Mitragotri, S.: 'Shape induced inhibition of phagocytosis of polymer particles', *Pharm. Res.*, 2009, **26**, (1), pp. 244–249
[98] Geng, Y., Dalhaimer, P., Cai, S., *et al.*: 'Shape effects of filaments versus spherical particles in flow and drug delivery', *Nat. Nanotechnol.*, 2007, **2**, (4), p. 249
[99] Sadeghi, B., Garmaroudi, F.S., Hashemi, M., *et al.*: 'Comparison of the anti-bacterial activity on the nanosilver shapes: nanoparticles, nanorods and nanoplates', *Adv. Powder Technol.*, 2012, **23**, (1), pp. 22–26
[100] Janát-Amsbury, M., Ray, A., Peterson, C., *et al.*: 'Geometry and surface characteristics of gold nanoparticles influence their biodistribution and uptake by macrophages', *Eur. J. Pharm. Biopharm.*, 2011, **77**, (3), pp. 417–423
[101] Pal, S., Tak, Y.K., Song, J.M.: 'Does the antibacterial activity of silver nanoparticles depend on the shape of the nanoparticle? A study of the gram-negative bacterium *Escherichia coli*', *Appl. Environ. Microbiol.*, 2007, **73**, (6), pp. 1712–1720
[102] Kavitha, T., Yuvaraj, H.: 'A facile approach to the synthesis of high-quality NiO nanorods: electrochemical and antibacterial properties', *J. Mater. Chem.*, 2011, **21**, (39), pp. 15686–15691
[103] Pang, H., Lu, Q., Li, Y., *et al.*: 'Facile synthesis of nickel oxide nanotubes and their antibacterial, electrochemical and magnetic properties', *Chem. Commun.*, 2009, **48**, (48), pp. 7542–7544
[104] Amna, T., Hassan, M.S., Yousef, A., *et al.*: 'Inactivation of foodborne pathogens by NiO/TiO_2 composite nanofibers: a novel biomaterial system', *Food Bioprocess Technol.*, 2013, **6**, (4), pp. 988–996
[105] Jan, T., Iqbal, J., Ismail, M., *et al.*: 'Eradication of multi-drug resistant bacteria by Ni doped ZnO nanorods: structural, Raman and optical characteristics', *Appl. Surf. Sci.*, 2014, **308**, pp. 75–81
[106] Kong, Y., Peng, J., Xin, Z., *et al.*: 'Selective synthesis and novel properties of single crystalline α-$CoMoO_4$ nanorods/nanowhiskers', *Mater. Lett.*, 2007, **61**, (10), pp. 2109–2112
[107] Kumar, P., Agnihotri, S., Roy, I.: 'Preparation and characterization of superparamagnetic iron oxide nanoparticles for magnetically guided drug delivery', *Int. J. Nanomed.*, 2018, **13**, (T-NANO 2014 Abstracts), pp. 43–46
[108] Sahoo, J.K., Paikra, S.K., Mishra, M., *et al.*: 'Amine functionalized magnetic iron oxide nanoparticles: synthesis, antibacterial activity and rapid removal of Congo red dye', *J. Mol. Liq.*, 2019, **282**, pp. 428–440
[109] Chapot-Chartier, M.-P., Kulakauskas, S.: 'Cell wall structure and function in lactic acid bacteria', *Microb. Cell Factories*, 2014, **13**, (1), p. S9
[110] Sohlenkamp, C., Geiger, O.: 'Bacterial membrane lipids: diversity in structures and pathways', *FEMS Microbiol. Rev.*, 2016, **40**, (1), pp. 133–159
[111] Rojas, E.R., Billings, G., Odermatt, P.D., *et al.*: 'The outer membrane is an essential load-bearing element in Gram-negative bacteria', *Nature*, 2018, **559**, (7715), p. 617
[112] Silhavy, T.J., Kahne, D., Walker, S.: 'The bacterial cell envelope', *Cold Spring Harbor Perspect. Biol.*, 2010, **2**, (5), p. a000414
[113] Epand, R.M., Walker, C., Epand, R.F., *et al.*: 'Molecular mechanisms of membrane targeting antibiotics', *Biochim. Biophys. Acta, Biomembr.*, 2016, **1858**, (5), pp. 980–987
[114] Thill, A., Zeyons, O., Spalla, O., *et al.*: 'Cytotoxicity of CeO_2 nanoparticles for *Escherichia coli*. Physico-chemical insight of the cytotoxicity mechanism', *Environ. Sci. Technol.*, 2006, **40**, (19), pp. 6151–6156
[115] Arakha, M., Pal, S., Samantarrai, D., *et al.*: 'Antimicrobial activity of iron oxide nanoparticle upon modulation of nanoparticle-bacteria interface', *Sci. Rep.*, 2015, **5**, p. 14813
[116] Argueta-Figueroa, L., Torres-Gómez, N., García-Contreras, R., *et al.*: 'Hydrothermal synthesis of pyrrhotite (Fex-1S) nanoplates and their antibacterial, cytotoxic activity study', *Prog. Nat. Sci., Mater. Int.*, 2018, **28**, (4), pp. 447–455
[117] Christena, L.R., Mangalagowri, V., Pradheeba, P., *et al.*: 'Copper nanoparticles as an efflux pump inhibitor to tackle drug resistant bacteria', *RSC Adv.*, 2015, **5**, (17), pp. 12899–12909
[118] Yuan, G., Cranston, R.: 'Recent advances in antimicrobial treatments of textiles', *Tex. Res. J.*, 2008, **78**, (1), pp. 60–72
[119] Nayak, P.S., Pradhan, S., Arakha, M., *et al.*: 'Silver nanoparticles fabricated using medicinal plant extracts show enhanced antimicrobial and selective cytotoxic propensities', *IET Nanobiotechnol.*, 2018, **13**, (2), pp. 193–201
[120] Wang, D., Zhao, L., Ma, H., *et al.*: 'Quantitative analysis of reactive oxygen species photogenerated on metal oxide nanoparticles and their bacteria toxicity: the role of superoxide radicals', *Environ. Sci. Technol.*, 2017, **51**, (17), pp. 10137–10145
[121] Khan, F.U., Chen, Y., Khan, N.U., *et al.*: 'Visible light inactivation of *E. coli*, cytotoxicity and ROS determination of biochemically capped gold nanoparticles', *Microb. Pathog.*, 2017, **107**, pp. 419–424
[122] Arijit Kumar, C., Ruchira, C., Tarakdas, B.: 'Mechanism of antibacterial activity of copper nanoparticles', *Nanotechnology*, 2014, **25**, (13), p. 135101
[123] Zhang, Y.-M., Rock, C.O.: 'Membrane lipid homeostasis in bacteria', *Nat. Rev. Microbiol.*, 2008, **6**, p. 222

[124] Lambert, A.J., Brand, M.D.: 'Reactive oxygen species production by mitochondria', in Stuart, J.A. (Ed.): '*Mitochondrial DNA*' (Springer, USA, 2009), pp. 165–181

[125] Liu, S., Li, M., Li, S., *et al.*: 'Synthesis and adsorption/photocatalysis performance of pyrite FeS_2', *Appl. Surf. Sci.*, 2013, **268**, pp. 213–217

[126] Outten, F.W., Wood, M.J., Muñoz, F.M., *et al.*: 'The SufE protein and the SufBCD complex enhance SufS cysteine desulfurase activity as part of a sulfur transfer pathway for Fe-S cluster assembly in *E. coli*', *J. Biol. Chem.*, 2003, **278**, (46), pp. 45713–45719

[127] Yao, Y., Lu, F., Zhu, Y., *et al.*: 'Magnetic core–shell $CuFe_2O_4@C_3N_4$ hybrids for visible light photocatalysis of Orange II', *J. Hazardous Mater.*, 2015, **297**, pp. 224–233

[128] Hou, X., Ma, H., Liu, F., *et al.*: 'Synthesis of Ag ion-implanted TiO_2 thin films for antibacterial application and photocatalytic performance', *J. Hazardous Mater.*, 2015, **299**, pp. 59–66

[129] Nino-Martinez, N., Martinez-Castanon, G., Aragon-Pina, A., *et al.*: 'Characterization of silver nanoparticles synthesized on titanium dioxide fine particles', *Nanotechnology*, 2008, **19**, (6), p. 065711

[130] Rawat, J., Rana, S., Srivastava, R., *et al.*: 'Antimicrobial activity of composite nanoparticles consisting of titania photocatalytic shell and nickel ferrite magnetic core', *Mater. Sci. Eng., C*, 2007, **27**, (3), pp. 540–545

[131] Chen, W.J., Tsai, P.J., Chen, Y.C.: 'Functional Fe_3O_4/TiO_2 core/shell magnetic nanoparticles as photokilling agents for pathogenic bacteria', *Small*, 2008, **4**, (4), pp. 485–491

[132] Pageni, P., Yang, P., Bam, M., *et al.*: 'Recyclable magnetic nanoparticles grafted with antimicrobial metallopolymer-antibiotic bioconjugates', *Biomaterials*, 2018, **178**, 363–372

[133] Kansara, K., Patel, P., Shukla, R.K., *et al.*: 'Synthesis of biocompatible iron oxide nanoparticles as a drug delivery vehicle', *Int. J. Nanomed.*, 2018, **13**, p. 79

[134] Patil, R.M., Thorat, N.D., Shete, P.B., *et al.*: 'Comprehensive cytotoxicity studies of superparamagnetic iron oxide nanoparticles', *Biochem. Biophys. Rep.*, 2018, **13**, pp. 63–72

[135] Feng, Q., Liu, Y., Huang, J., *et al.*: 'Uptake, distribution, clearance, and toxicity of iron oxide nanoparticles with different sizes and coatings', *Sci. Rep.*, 2018, **8**, (1), p. 2082

[136] Tran, P.A., Nguyen, H.T., Fox, K., *et al.*: '*In vitro* cytotoxicity of iron oxide nanoparticles: effects of chitosan and polyvinyl alcohol as stabilizing agents', *Mater. Res. Express*, 2018, **5**, (3), p. 035051

[137] Haberl, N., Hirn, S., Wenk, A., *et al.*: 'Cytotoxic and proinflammatory effects of PVP-coated silver nanoparticles after intratracheal instillation in rats', *Beilstein J. Nanotechnol.*, 2013, **4**, p. 933

[138] Khayatian, S.A., Kompany, A., Shahtahmassebi, N., *et al.*: 'Preparation and characterization of Al doped ZnO NPs/graphene nanocomposites synthesized by a facile one-step solvothermal method', *Ceram. Int.*, 2016, **42**, (1), pp. 110–115

[139] Feng, L., Zhang, S., Liu, Z.: 'Graphene based gene transfection', *Nanoscale*, 2011, **3**, (3), pp. 1252–1257

[140] Kassaee, M.Z., Motamedi, E., Majdi, M.: 'Magnetic Fe_3O_4-graphene oxide/polystyrene: fabrication and characterization of a promising nanocomposite', *Chem. Eng. J.*, 2011, **172**, (1), pp. 540–549

[141] Mahmoodabadi, A.N., Kompany, A., Mashreghi, M.: 'Characterization, antibacterial and cytotoxicity studies of graphene-Fe_3O_4 nanocomposites and Fe_3O_4 nanoparticles synthesized by a facile solvothermal method', *Mater. Chem. Phys.*, 2018, **213**, pp. 285–294

[142] Allafchian, A., Jalali, S.A.H., Bahramian, H., *et al.*: 'Preparation, characterization, and antibacterial activity of $NiFe_2O_4$/PAMA/Ag–TiO_2 nanocomposite', *J. Magn. Magn. Mater.*, 2016, **404**, pp. 14–20

[143] Mosaiab, T., Jeong, C.J., Shin, G.J., *et al.*: 'Recyclable and stable silver deposited magnetic nanoparticles with poly (vinyl pyrrolidone)-catechol coated iron oxide for antimicrobial activity', *Mater. Sci. Eng., C*, 2013, **33**, (7), pp. 3786–3794

[144] Mosmann, T.: 'Rapid colorimetric assay for cellular growth and survival: application to proliferation and cytotoxicity assays', *J. Immunol. Methods*, 1983, **65**, (1–2), pp. 55–63

[145] Slater, T.F., Sawyer, B., Sträuli, U.: 'Studies on succinate-tetrazolium reductase systems: III. Points of coupling of four different tetrazolium salts III. Points of coupling of four different tetrazolium salts', *Biochim. Biophys. Acta*, 1963, **77**, pp. 383–393

[146] Altman, F.P.: 'Tetrazolium salts and formazans', *Prog. Histochem. Cytochem.*, 1976, **9**, (3), p. III-51

[147] Burdon, R.H., Gill, V., Rice-evans, C.: 'Reduction of a Tetrazolium salt and superoxide generation in human tumor cells (HeLa)', *Free Radic. Res. Commun.*, 1993, **18**, (6), pp. 369–380

[148] Sandle, T.: '14 – antibiotics and preservatives', in Sandle, T. (Ed.): '*Pharmaceutical microbiology*' (Woodhead Publishing, Cambridge, UK, 2016), pp. 171–183

[149] Wiegand, I., Hilpert, K., Hancock, R.E.: 'Agar and broth dilution methods to determine the minimal inhibitory concentration (MIC) of antimicrobial substances', *Nat. Protocol*, 2008, **3**, (2), p. 163

[150] Ansari, M.A., Baykal, A., Asiri, S., *et al.*: 'Synthesis and characterization of antibacterial activity of spinel chromium-substituted copper ferrite nanoparticles for biomedical application', *J. Inorg. Organomet. Polym. Mater.*, 2018, **28**, (6), pp. 1–12

[151] Allafchian, A.R., Jalali, S., Amiri, R., *et al.*: 'Synthesis and characterization of the $NiFe_2O_4$@ TEOS–TPS@Ag nanocomposite and investigation of its antibacterial activity', *Appl. Surf. Sci.*, 2016, **385**, pp. 506–514

[152] Allafchian, A.R., Jalali, S.A.H., Amiri, R., *et al.*: 'Antibacterial activity of new magnetic Ag/TiO_2 nanocomposite in silane sol–gel matrix', *J. Mater. Sci., Mater. Electron.*, 2017, **28**, (16), pp. 12312–12319

[153] Lewinski, N., Colvin, V., Drezek, R.: 'Cytotoxicity of nanoparticles', *Small*, 2008, **4**, (1), pp. 26–49

[154] Riccardi, C., Nicoletti, I.: 'Analysis of apoptosis by propidium iodide staining and flow cytometry', *Nat. Protocol*, 2006, **1**, (3), p. 1458

[155] Gong, P., Li, H., He, X., *et al.*: 'Preparation and antibacterial activity of Fe_3O_4@Ag nanoparticles', *Nanotechnology*, 2007, **18**, (28), p. 285604

[156] Reddy, K.M., Feris, K., Bell, J., *et al.*: 'Selective toxicity of zinc oxide nanoparticles to prokaryotic and eukaryotic systems', *Appl. Phys. Lett.*, 2007, **90**, (21), p. 213902

[157] AshaRani, P.V., Low Kah Mun, G., Hande, M.P., *et al.*: 'Cytotoxicity and genotoxicity of silver nanoparticles in human cells', *ACS Nano*, 2009, **3**, (2), pp. 279–290

[158] Lu, C.-W., Hung, Y., Hsiao, J.-K., *et al.*: 'Bifunctional magnetic silica nanoparticles for highly efficient human stem cell labeling', *Nano Lett.*, 2007, **7**, (1), pp. 149–154

[159] Liu, S., Huang, G., Yu, J., *et al.*: 'Porous fluorinated SnO_2 hollow nanospheres: transformative self-assembly and photocatalytic inactivation of bacteria', *ACS Appl. Mater. Interfaces*, 2014, **6**, (4), pp. 2407–2414

[160] Qin, P., Chen, C., Wang, Y., *et al.*: 'A facile method for synthesis of silver and Fe_3O_4 reusable hierarchical nanocomposite for antibacterial applications', *J. Nanosci. Nanotechnol.*, 2017, **17**, (12), pp. 9350–9355

[161] Ma, S., Zhan, S., Jia, Y., *et al.*: 'Superior antibacterial activity of Fe_3O_4–TiO_2 nanosheets under solar light', *ACS Appl. Mater. Interfaces*, 2015, **7**, (39), pp. 21875–21883

[162] Tran, N., Webster, T.J.: 'Effects of magnetite and maghemite nanoparticles on bone cell and *Staphylococcus aureus* functions', *Technol. Innov.*, 2011, **13**, (1), pp. 39–50

[163] Malwal, D., Gopinath, P.: 'Efficient adsorption and antibacterial properties of electrospun CuO-ZnO composite nanofibers for water remediation', *J. Hazardous Mater.*, 2017, **321**, pp. 611–621

[164] Wang, C., Xu, S., Zhang, K., *et al.*: 'Streptomycin-modified Fe_3O_4–Au@Ag core–satellite magnetic nanoparticles as an effective antibacterial agent', *J. Mater. Sci.*, 2017, **52**, (3), pp. 1357–1368

[165] Li, M., Liu, L.Q., Xi, N., *et al.*: 'Nanoscale monitoring of drug actions on cell membrane using atomic force microscopy', *Acta Pharmacol. Sin.*, 2015, **36**, (7), p. 769

[166] Liu, J.L., Luo, Z., Bashir, S.: 'A progressive approach on inactivation of bacteria using silver–titania nanoparticles', *Biomater. Sci.*, 2013, **1**, (2), pp. 194–201

[167] Yong, Y.C., Wang, Y.Z., Zhong, J.J.: 'Nano-spectroscopic imaging of proteins with near-field scanning optical microscopy (NSOM)', *Curr. Opin. Biotechnol.*, 2018, **54**, pp. 106–113

[168] Laborda, F., Bolea, E., Cepriá, G., *et al.*: 'Detection, characterization and quantification of inorganic engineered nanomaterials: a review of techniques and methodological approaches for the analysis of complex samples', *Anal. Chim. Acta*, 2016, **904**, pp. 10–32

[169] Patil, S., Naik, H.B., Nagaraju, G., *et al.*: 'Sugarcane juice mediated eco-friendly synthesis of visible light active zinc ferrite nanoparticles: application to degradation of mixed dyes and antibacterial activities', *Mater. Chem. Phys.*, 2018, **212**, pp. 351–362

[170] Karunakaran, C., Vinayagamoorthy, P.: 'Synthesis, electrical, magnetic, optical and bactericidal properties and enhanced photocatalytic activity of Ag-decorated $ZnFe_2O_4$-dispersed ZnO nanoflakes', *Surf. Interfaces*, 2018, **10**, pp. 123–128

[171] Fadley, C.S.: 'X-ray photoelectron spectroscopy: progress and perspectives', *J. Electron Spectrosc. Relat. Phenom.*, 2010, **178–179**, pp. 2–32

[172] Rayegan, A., Allafchian, A., Sarsari, I.A., *et al.*: 'Synthesis and characterization of basil seed mucilage coated Fe_3O_4 magnetic nanoparticles as a drug carrier for the controlled delivery of cephalexin', *Int. J. Biol. Macromol.*, 2018, **113**, pp. 317–328

[173] Roggo, Y., Chalus, P., Maurer, L., *et al.*: 'A review of near infrared spectroscopy and chemometrics in pharmaceutical technologies', *J. Pharm. Biomed. Anal.*, 2007, **44**, (3), pp. 683–700

[174] Yu, S., Li, G., Liu, R., *et al.*: 'Dendritic Fe_3O_4@Poly(dopamine)@PAMAM nanocomposite as controllable no-releasing material: a synergistic photothermal and no antibacterial study', *Adv. Funct. Mater.*, 2018, **28**, (20), p. 1707440

[175] Whyman, G., Bormashenko, E., Stein, T.: 'The rigorous derivation of Young, Cassie–Baxter and Wenzel equations and the analysis of the contact angle hysteresis phenomenon', *Chem. Phys. Lett.*, 2008, **450**, (4), pp. 355–359

[176] Eral, H.B., 't Mannetje, D.J.C.M., Oh, J.M.: 'Contact angle hysteresis: a review of fundamentals and applications', *Colloid Polym. Sci.*, 2013, **291**, (2), pp. 247–260

[177] Sangeetha, J., Philip, J.: 'Synthesis, characterization and antimicrobial property of Fe_3O_4-Cys-HNQ nanocomplex, with l-cysteine molecule as a linker', *RSC Adv.*, 2013, **3**, (21), pp. 8047–8057

[178] Yoksan, R., Chirachanchai, S.: 'Silver nanoparticle-loaded chitosan–starch based films: fabrication and evaluation of tensile, barrier and antimicrobial properties', *Mater. Sci. Eng., C*, 2010, **30**, (6), pp. 891–897

[179] Thukkaram, M., Sitaram, S., Kannaiyan, S.K., *et al.*: 'Antibacterial efficacy of iron-oxide nanoparticles against biofilms on different biomaterial surfaces', *Int. J. Biomater.*, 2014, **2014**, p. 6

[180] Nabila, M.I., Kannabiran, K.: 'Biosynthesis, characterization and antibacterial activity of copper oxide nanoparticles (CuO NPs) from actinomycetes', *Biocatal. Agric. Biotechnol.*, 2018, **15**, pp. 56–62

[181] Burchard, W.: '5 – dynamic light scattering', in Matricardi, P., Alhaique, F., Coviello, T. (Eds.): '*Polysaccharide hydrogels: characterization and biomedical applications*' (CRC Press, Boca Raton, FL, USA, 2016, 1st edn.), pp. 167–207

[182] Chai, M.H.H., Amir, N., Yahya, N., *et al.*: 'Characterization and colloidal stability of surface modified zinc oxide nanoparticle', *J. Phys., Conf. Ser.*, 2018, **1123**, (1), p. 012007

[183] Spulber, R., Chifiriuc, C., Fleancu, M., *et al.*: 'Antibacterial activity of magnetite nanoparticles coated with bee pollen extracts'. 'Agriculture for Life, Life for Agriculture' Conf. Proc., 2018, pp. 579–585